Renewable and Sustainable Energy Reviews 195 (2024) 114333

Contents lists available at ScienceDirect

Renewable and Sustainable Energy Reviews

journal homepage: www.elsevier.com/locate/rser

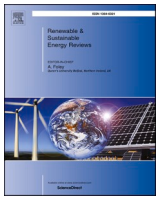

Upcycling of plastic wastes for hydrogen production: Advances and perspectives

Zhijie Chen [a], Wei Wei [a], Xueming Chen [b], Yiwen Liu [a], Yansong Shen [c], Bing-Jie Ni [a,*]

[a] Centre for Technology in Water and Wastewater, School of Civil and Environmental Engineering, University of Technology Sydney, Sydney, NSW, 2007, Australia
[b] Fujian Provincial Engineering Research Center of Rural Waste Recycling Technology, College of Environment and Safety Engineering, Fuzhou University, Fuzhou, Fujian, 350116, China
[c] School of Chemical Engineering, University of New South Wales, Sydney, NSW, 2052, Australia

ARTICLE INFO

Keywords:
Plastic wastes
Upcycling
Pyrolysis
Thermochemical conversion
Composites
Catalysis
Hydrogen energy
Photocatalysts
Electrocatalysts
Waste utilization

ABSTRACT

The abundant plastic wastes become an imperative global issue, and how to handle these organic wastes gains growing scientific and industrial interest. Recently, converting plastic wastes into hydrogen fuel has been investigated, and the "waste-to-value" practice accelerates the circular economy. To accelerate the development of plastic-to-hydrogen conversion, in this review, recent advances in plastic-to-hydrogen conversion via thermochemical, photocatalytic, and electrocatalytic routes are analyzed. All of the thermo-, photo-, and electrochemical processes can transform different plastic wastes into hydrogen, and the hydrogen production efficiency depends heavily on the selected techniques, operating parameters, and applied catalysts. The application of rational-designed catalysts can promote the selective production of hydrogen from plastic feedstocks. Further studies on process optimization, cost-effective catalyst design, and mechanism investigation are needed.

1. Introduction

The ubiquitous plastics are important for human daily lives and many industries because of their high corrosion resistance, high strength-to-weight ratio, tunable functionality, good flexibility, and facile processability [1–3]. The speedily growing fabrication/utilization and inappropriate treatment of plastic products lead to a large number of plastic wastes (especially microplastics), which is an alarming environmental and social issue [4–6]. As predicted, ~8.3 billion tons of non-biodegradable plastics have been generated, and over 75% of them are discarded as wastes [7]. It is thus urgent to manage abundant plastic wastes [8,9]. Conventionally, incineration and landfilling are two universal techniques for plastic waste treatment, resulting in grave environmental deterioration [10–12]. As an alternative, converting annoying plastic wastes into value-added fuels (e.g., hydrogen) gains intensive interest due to the prominent importance of hydrogen energy in realizing the carbon neutrality goal [7,13].

Upcycling plastic wastes into hydrogen gas involves the breakdown of long hydrocarbon chains under typical physical or chemical conditions, e.g., high temperature, light field, and electric field [7]. Thermochemical conversion is the most widely used method for plastic-to-hydrogen upcycling, including pyrolysis, gasification, etc. The hydrogen production efficiency is highly dependent on the involved thermochemical processes and reaction conditions (e.g., temperature, time, pressure, atmosphere, functional materials, and plastic feedstock) [14]. For instance, the utilization of Ni/MCM-41 catalyst can attain a

Abbreviations: CB, Conduction band; CER, Chlorine evolution reaction; CGE, Carbon gasification efficiencies; CN, Carbon nitride; CNT, Carbon nanotube; CPD, Carbonized polymer dots; CSBR, Conical spouted bed reactor; CSMP, Continuous-stirred microwave pyrolysis; EG, Ethylene glycol; ER, Equivalence ratio; EGOR, Ethylene glycol oxidation reaction; FBR, Fluidized bed reactor; FE, Faradaic efficiency; GC, Gas chromatography; GFRP, Glass fiber-reinforced plastic; GOR, Glycerol oxidation reaction; HDPE, High density polyethylene; HER, Hydrogen evolution reaction; HGE, Hydrogen gasification efficiencies; LDPE, Low density polyethylene; MEA, Membrane-electrode assembly; MOF, Metal–organic framework; MSW, Municipal solid waste; NHE, Normal hydrogen electrode; OER, Oxygen evolution reaction; PE, Polyethylene; PEC, Photoelectrochemical; PET, Polyethylene terephthalate; PLA, Polylactic acid; PMMA, Poly(methyl methacrylate); PP, Polypropylene; PS, Polystyrene; PUR, Polyurethane; PVC, Polyvinyl chloride; rGO, Reduced graphene oxide; SCW, Supercritical water; SCWG, Supercritical water gasification; T, Temperature; TPA, Terephthalic acid; UOS, University of Seoul; VB, Valence band; WGS, Water gas shift.

* Corresponding author.
E-mail address: bingjieni@gmail.com (B.-J. Ni).

https://doi.org/10.1016/j.rser.2024.114333
Received 15 March 2023; Received in revised form 5 February 2024; Accepted 18 February 2024
Available online 27 February 2024

Table 1
Representative achievements in thermochemical upcycling of plastics for hydrogen fuel. (PS: polystyrene; T: temperature; PP: polypropylene; HDPE: high density polyethylene; PE: polyethylene; LDPE: low density polyethylene; MSW: municipal solid waste).

Thermochemical technique	Plastic	Reaction conditions	Hydrogen production performance
Pyrolysis-catalytic steam reforming [32]	PS	T (pyrolysis): 500 °C; T (reforming): 800 °C; Water flow rate (reforming): 6 g h^{-1}; Catalyst (reforming): Ni/Al_2O_3	H_2 yield: 62.26 mmol g_{PS}^{-1}
Pyrolysis-catalytic steam gasification [33]	PP	T (pyrolysis): 500 °C; T (reforming): 800 °C; Water flow rate (reforming): 4.74 g h^{-1}; Catalyst (gasification): Ni–Mn–Al	H_2 yield: 71.4 mmol g_{PP}^{-1}
Flash pyrolysis-steam reforming [34]	HDPE	Plastic feeding speed: 5 g min^{-1}; Steam/plastic ratio: 5; T (pyrolysis): 500 °C; T (reforming): 700 °C; Space time: 16.7 g_{cat} min g_{HDPE}^{-1}; Catalyst: Ni	H_2 yield: 0.381 g g_{HDPE}^{-1}
Plasma-catalytic pyrolysis [35]	PP	T (pyrolysis): 400 °C; Plasma power: 120 W; Catalyst: zeolite ZSM-5; Catalyst/plastic ratio: 2	H_2 yield: 4.19 mmol g_{PP}^{-1}
Microwave-catalytic pyrolysis [36]	PE	Microwave power: 900 W; Time: 6 min; Catalyst: $FeAlO_x$; Catalyst/plastic ratio: 1	H_2 yield: 48.1 mmol g_{PE}^{-1}
Microwave-catalytic pyrolysis [37]	HDPE	Microwave power: 1000 W; T: 700–800 °C; Time: 10 min; Catalyst: Fe/Ni–CeO_2@CNTs; Catalyst/plastic ratio: 1.67	H_2 yield: 50.2 mmol g_{HDPE}^{-1}
Two-stage air gasification [38]	PP and LDPE	T (1st stage): 600 °C; T (2nd stage): 800 °C: 800 °C; Equivalence ratio: 0.1; Catalyst (1st stage): Ni/Al-SBA-15; Catalyst (2nd stage): Ni–Cu/CaO–SiO_2	H_2 yield: 857.6 mmol g_{cat}^{-1}
Steam gasification [39]	MSW	Feed rate: 0.13 kg h^{-1}; Steam flow rate: 0.16 kg h^{-1}; T: 800 °C; Catalyst: NiO/modified dolomite; Steam/MSW: 1.23	H_2 yield: 40.02 mmol g_{MSW}^{-1}
Steam gasification [40]	Mixed plastics	Steam flow rate: 0.3 kg h^{-1}; T: 900 °C; Time: 10 min; Catalyst: CaO; Catalyst/plastic ratio: 1	H_2 yield: 104 mmol $g_{plastic}^{-1}$
Supercritical water gasification [41]	PP and lignite	PP/lignite ratio: 1; Feed concentration of waste: 10 wt%; T: 800 °C; Time: 30 min	H_2 yield: 24.17 mmol g_{waste}^{-1}
Supercritical water gasification [42]	Waste tires	Feed concentration of waste: 5 wt%; T: 625 °C; Time: 60 min; Catalyst: Ni/SiO_2–Al_2O_3	H_2 yield: 19.7 mmol $g_{plastic}^{-1}$
Supercritical water gasification [43]	PE and soda lignin	PP/soda lignin ratio: 1; Feed concentration of waste: 5 wt%; T: 700 °C; Time: 30 min; Catalyst: NaOH	H_2 yield: 63.3 mmol g_{waste}^{-1}
Nonthermal atmospheric plasma treatment [44]	LDPE	Flow rate: 2 slpm; Voltage level: 75%; Electrode-feedstock spacing: 5 mm; Time: 10 min	H_2 yield: 0.42 mmol g_{LDPE}^{-1}
Thermal plasma steam gasification [45]	HDPE and biomass	HDPE/biomass ratio: 4; Plasma power: 22 kW; T: 600 °C; Steam/carbon flow ratio: 1; Time: 20 min	H_2 yield: 78.55 mmol g_{waste}^{-1}

higher hydrogen evolution value (18 mmol $g_{plastic}^{-1}$) than Ni/Y-zeolite, Ni/Mo_2C, and $Ni/BaTiO_3$ in a pyrolysis-catalytic steam reforming process [15]. The rational design of thermochemical processes and catalysts is thus important for efficient hydrogen production from plastic wastes, and recent achievements achieved in this field have significantly accelerated the upcycling of plastic wastes and the hydrogen economy.

Aside from conventional thermochemical methods, photo-reforming and electro-reforming are emerging techniques for plastic waste valorization. Photo-reforming (photolysis, photocatalysis) has been extensively used for chemical reactions, such as water electrolysis and pollutant degradation, and the exploitation of solar energy for emerging plastic conversion provides a green and facile method to valorize plastic feedstocks for sustainable hydrogen production. Typically, a photochemical reaction needs the application of a semiconductor material as the photocatalyst, which produces photoexcited electron-hole pairs as active reaction sites to initiate the redox reaction under light radiation [16]. Current efforts have witnessed the development of a group of high-performance photocatalysts, such as oxides, sulfides, and carbon materials, and novel photo-reaction systems for plastic-to-hydrogen conversion [17]. Compared with photo-reforming, electro-reforming is a more kinetically favorable process due to the highly flexible energy input. A group of studies has employed plastic wastes as the substrate for hydrogen production under an electric field. The hydrogen production efficiency of plastic electro-reforming is more efficient than conventional water electrolysis due to the lower energy barrier of plastic electrooxidation than oxygen evolution reaction (OER) [18]. Thus, the plastic electro-reforming process can realize energy-saving hydrogen production and waste valorization simultaneously.

The upcycling of plastic wastes has been extensively studied and reviewed. Currently, several informative reviews have summarized the upcycling of plastic wastes into carbon materials, fuels, and chemicals [19–29], but the emphasis is not on hydrogen production. One recent review focuses on plastic-to-hydrogen conversion with thermochemical processes [30], while a comprehensive review that analyzes plastic waste upcycling for hydrogen gas production is still lacking. The great interest in this topic thus urges a systematical review covering diverse techniques for plastic-to-hydrogen upcycling, including conversion processes, reaction mechanisms, reactors, advanced catalysts, etc.

Herein, this review aims to make a thorough effort to analyze current advances in the conversion of plastic wastes into hydrogen fuel. The application of advanced techniques, associated with related reactors, reaction mechanisms, and key functional materials (catalysts) in thermochemical conversion, photo-reforming, and electrochemical-reforming are detailed successively. The techniques and/or functional materials-dependent hydrogen production efficiency will be emphasized. Future perspectives of this booming field are also proposed.

2. Thermochemical conversion

Thermochemical conversion is the most prominent method for plastic-to-hydrogen upcycling, and generally, syngas (gas mixture of H_2, CO, CO_2, etc.) instead of pure hydrogen gas is obtained. Pyrolysis (plastics converted in an inert atmosphere) and gasification (plastics converted under a controlled partial oxidation condition) are the main implemented thermochemical methods [31]. Hydrogen production efficiency is highly related to the thermochemical technique, plastic feedstock, catalyst, reaction temperature, pressure, and time. In this section, current efforts made in thermochemically recovering hydrogen fuel from plastic wastes are discussed, and representative achievements in plastics-to-hydrogen upcycling are listed in Table 1.

2.1. Pyrolysis

Pyrolysis is the most widely used thermochemical process for converting plastic wastes into value-added hydrogen fuel [46]. Pyrolysis of plastic is the process of thermally degrading long chain polymer

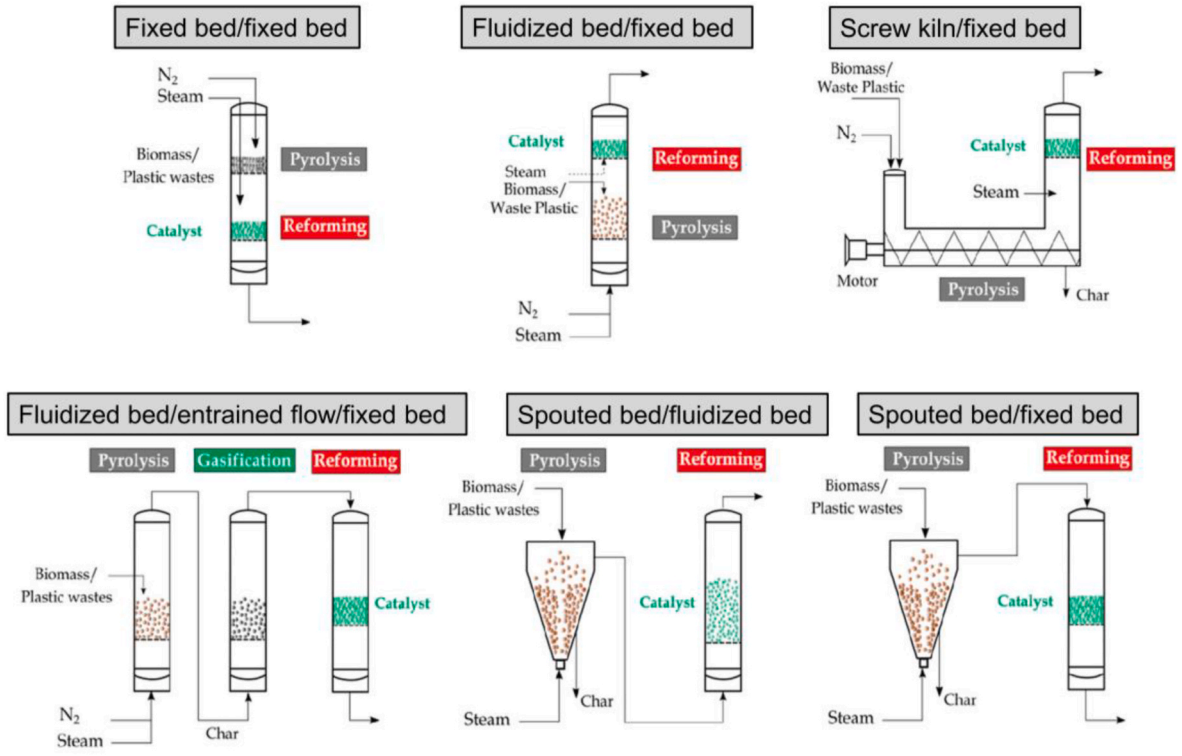

Fig. 1. General reactor configurations for plastic thermal pyrolysis-catalytic reforming for hydrogen production. Reproduced with permission from Ref. [48] Copyright 2021 American Chemical Society.

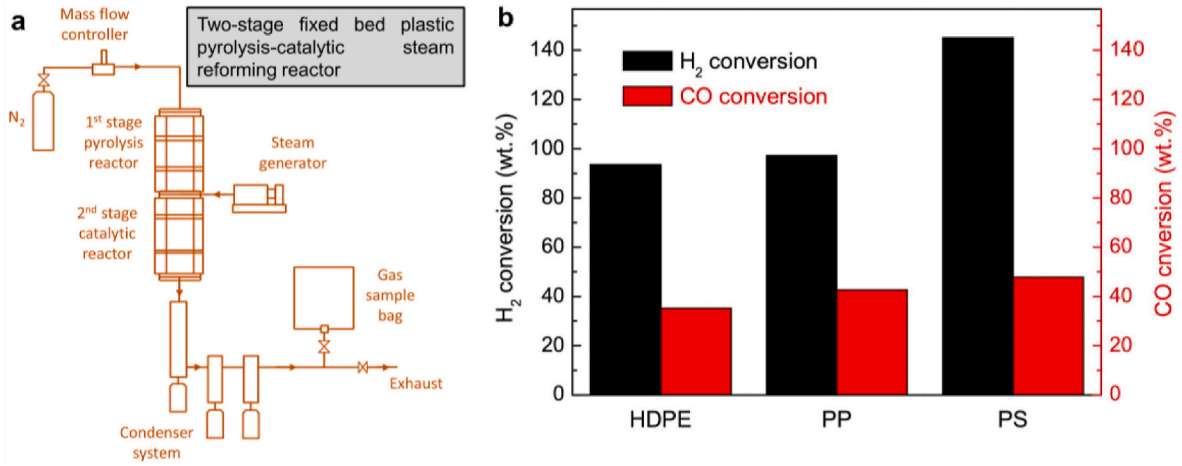

Fig. 2. (a) Illustration of the two-stage fixed bed pyrolysis-catalytic steam reforming reactor. (b) The conversion of different plastics with the Ni/Al_2O_3 catalyst (HDPE: high density polyethylene, PP: polypropylene, PS: polystyrene). Reproduced with permission from Ref. [32] Copyright 2018 Elsevier.

molecules into smaller, less complex molecules through heat and pressure [11]. The process requires intense heat with a shorter duration and in the absence of oxygen. In addition, pyrolysis is highly flexible since the process parameters can be manipulated to optimize the hydrogen yield [47]. For plastic-to-hydrogen conversion, the most widely used pyrolysis-based techniques include thermal pyrolysis-catalytic steam reforming, catalytic pyrolysis, and microwave pyrolysis.

2.1.1. *Thermal pyrolysis*

Thermal pyrolysis is a common pyrolysis type, which involves the upgrade of waste plastic upon heat treatment and under an inert atmosphere. This process involves heat application of the feedstock, in which the reaction temperatures range from 400 to 600 °C [47]. The thermal pyrolysis process occurs under the influence of inert conditions for the thermal breakdown of waste plastics into diverse products. Since this process does not utilize catalysts, a relatively high temperature and energy consumption is involved [46]. In addition, thermal pyrolysis generally generates liquid products that constitute high boiling point-range hydrocarbons, leading to low-value products [32]. To address these issues, further processing is required to optimize thermal pyrolytic products into useful products. For plastic-to-hydrogen conversion, a catalytic steam reforming post-treatment is widely used after thermal pyrolysis to improve the hydrogen production efficiency [34].

The prominent thermal pyrolysis-catalytic steam reforming process (pyrolysis-gasification) contains two successive stages. In the first stage, plastic wastes are pyrolyzed at a relatively low temperature (~500 °C),

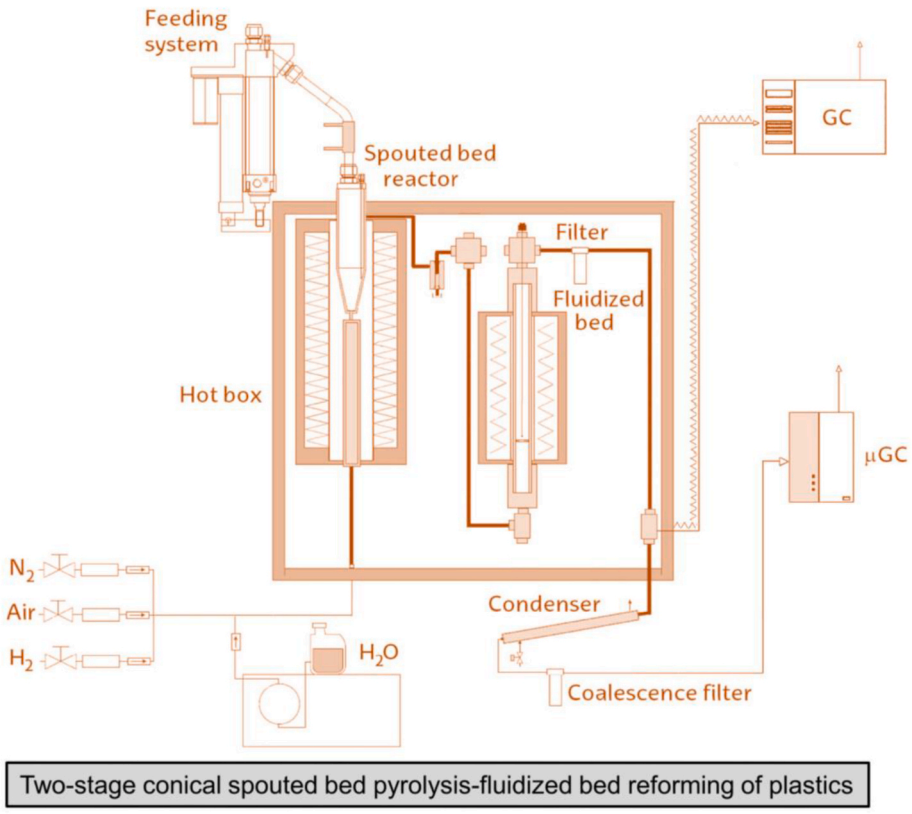

Fig. 3. Two-stage conical spouted bed pyrolysis-fluidized bed reforming of plastics (GC: gas chromatography). Reproduced with permission from Ref. [56] Copyright 2018 Elsevier.

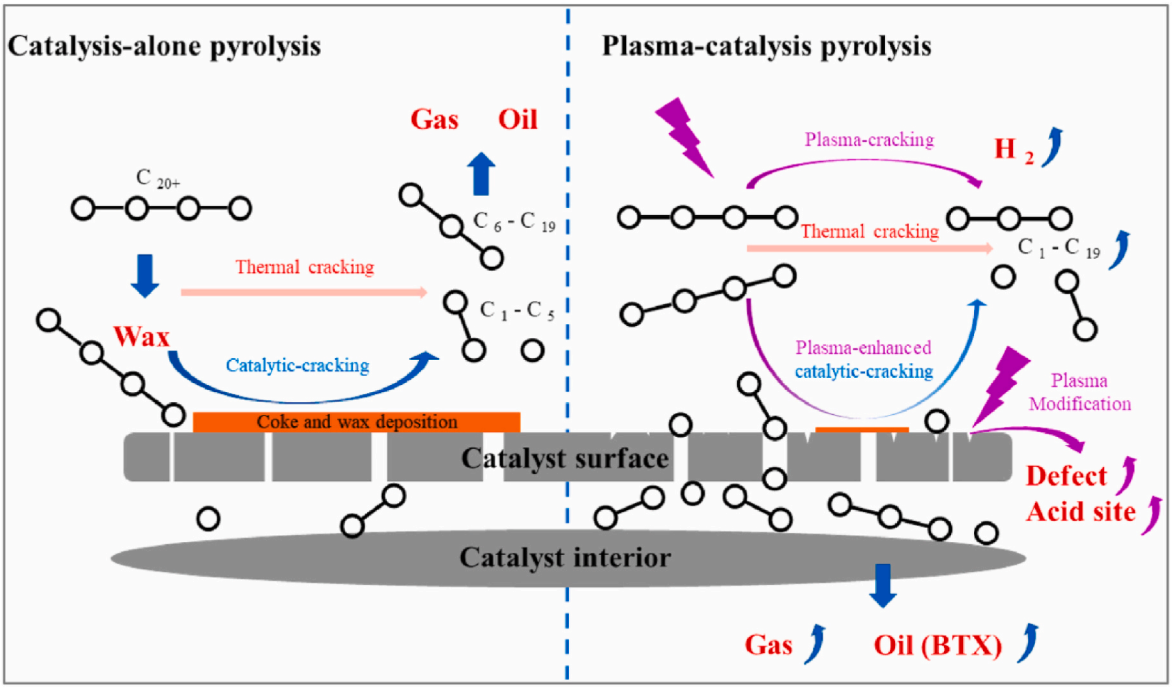

Fig. 4. Synergistic effect of plasma-catalysis pyrolysis in the upcycling of plastics (BTX: benzene, toluene, xylene). Reproduced with permission from Ref. [35] Copyright 2022 Elsevier.

which produces a mixture of hydrocarbon gases and vapors from plastics' decomposition. Then, the generated pyrolysis gases pass to the catalytic reactor (~800 °C, with steam and catalysts) for reforming to obtain hydrogen-rich gas [52]. The pyrolysis-catalytic reforming technique has evolved several sophisticated experimental configurations, such as fixed bed pyrolysis-fixed bed reforming, spouted bed

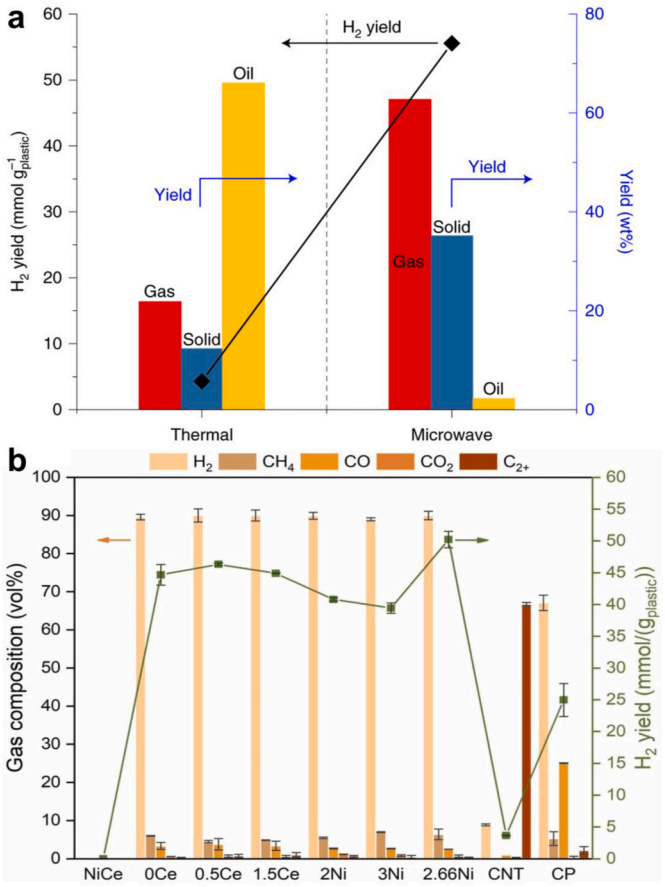

Fig. 5. (a) Comparison of microwave and conventional thermal pyrolysis in the upcycling of HDPE (HDPE: high density polyethylene). Reproduced with permission from Ref. [66] Copyright 2020 Springer Nature. (b) Gas product composition and hydrogen yield from HDPE by microwave pyrolysis over diverse catalysts and by conventional catalytic pyrolysis (CP: $Ni_{1.25}Ce_{0.5}$ catalyst, CNT: carbon nanotube). Reproduced with permission from Ref. [37] Copyright 2022 Elsevier.

pyrolysis-fluidized bed reforming, fluidized bed pyrolysis-fluidized bed reforming continuous system, and screw kiln pyrolysis-fixed bed reforming (Fig. 1) [53]. These setups have been successfully implemented for plastic-to-hydrogen upcycling, and many studies focus on the optimization of process parameters (e.g., catalyst properties, reactor design, reaction temperature, plastic species) for gaining hydrogen-rich gas products.

Fig. 2a shows a typical two-stage fixed bed plastic pyrolysis-catalytic steam reforming reactor, which contains a N_2 supply system, a two-stage stainless tube reactor, a steam generator, a gaseous product condensing system, and a gas collection/measurement system [32]. This reactor system shows the merits of simple design and operation and has been used for the conversion of diverse plastics in the batch regime. Using a Ni/Al_2O_3 catalyst, the two-stage fixed bed system can convert HDPE, PS, and PP into syngas. Compared to PP and HDPE, the PS feedstock leads to a higher hydrogen conversion rate (Fig. 2b), with 62.26 mmol H_2 g_{PS}^{-1} and 36.10 mmol CO g_{PS}^{-1} can be obtained. With this system, diverse Ni-based catalysts have been developed for plastic conversions, such as Fe–Ni–MCM-41 [49], NiMnAl catalyst [50], Ni/MCM-41 [51], Ni/zeolite [51,52], and Ni–Pt/TiO_2 [53]. It is suggested that catalysts' physicochemical properties (e.g., chemical composition, porosity, size) play a critical role in determining hydrogen yield and ratio in syngas. For instance, the application of the Ni–Mn–Al catalyst realizes a higher hydrogen yield (71.4 mmol H_2 $g_{plastic}^{-1}$) than Ni–Zn–Al (45.9 mmol H_2 $g_{plastic}^{-1}$), Ni–Ce–Al (63.1 mmol H_2 $g_{plastic}^{-1}$), and Ni–Ca–Al (68.5 mmol H_2 $g_{plastic}^{-1}$). The reason is that the strong interaction between the catalyst support and Ni results in higher hydrogen production [33]. This study also suggests that a higher steam injection rate benefits the hydrogen yield.

To further improve the pyrolysis-catalytic steam reforming system and makes it an automatic and continuous operation regime, a continuous feed of plastics into the two-stage reactor system has been developed [54]. The main feature is the incorporation of a continuous feeder and the packed-bed catalytic unit, which makes the reaction system a promising option for industrial applications. Park and co-authors found that a higher hydrogen yield could be obtained with the 5 wt% $Ru/\gamma\text{-}Al_2O_3$ catalyst (0.33–0.36 g H_2 g_{PP}^{-1}) compared to the 0.5 wt% $Ru/\gamma\text{-}Al_2O_3$ catalyst (0.03–0.04 g H_2 g_{PP}^{-1}) [55], while the reason remains unclear.

The introduction of spouted bed and fluidized bed reactors further improves the reaction efficiency of plastic waste conversion. As shown in Fig. 3, the continuous process contains a conical spouted bed reactor (CSBR, for pyrolysis) and a fluidized bed reactor (FBR, for reforming) [56]. Compared with fixed bed-involved systems which generally form coke deposition, the CSBR-FBR reactor can realize better heat/mass transfer efficiencies, shorter residence time, and more facile operations [57]. A study by Barbarias et al. found that plastic feedstock largely influenced the hydrogen production yield, increasing from polyethylene terephthalate (PET, 18.2 wt%) to PS (29.1 wt%) and polyolefins (34.8–37.3 wt%) [56]. The same group also studied the influence of reforming temperature, reforming space time, and steam/plastic (S/P) ratio on hydrogen production from HDPE, using a Ni catalyst. A rise in these parameters (S/P ratio of 5, reforming space time of 16.7 g_{cat} min g_{HDPE}^{-1}, and reforming temperature of 700 °C) boosts HDPE-derived volatile reforming, achieving a high hydrogen yield of 0.381 g H_2 g_{HDPE}^{-1} [34]. The study by Arregi et al. investigated the effect of catalyst properties and reforming space time on hydrogen production from polyolefinic waste plastics. Compared with $Ni/CeO_2–Al_2O_3$ and Ni/Al_2O_3, the La-doped $Ni/La_2O_3–Al_2O_3$ shows improved catalyst performance regarding high conversion efficiency (>99%), high hydrogen production ratio (34.9%) at a high reforming space time of 16.7 g_{cat} min g_{HDPE}^{-1}. The higher catalytic performance of $Ni/La_2O_3–Al_2O_3$ may result from the low coke deposition (2.24 wt%) [58].

2.1.2. Catalytic pyrolysis

Catalytic pyrolysis refers to the pyrolysis process that is carried out with the presence of catalysts. The process shows high potential for the conversion of plastic waste into hydrogen with enhanced efficiency as compared to conventional catalyst-free thermal pyrolysis [59,60]. The hydrogen production efficiency of the catalytic pyrolysis process is affected by catalysts, temperature, retention time, and feedstock composition. Generally, the production of hydrogen from plastic requires a high catalytic temperature of ~800 °C. Nevertheless, a high catalytic temperature tends to cause agglomeration of pyrolysis volatiles, catalyst deactivation, and high energy costs, ultimately limiting its application [61].

To address these issues, introducing plasma into the catalytic pyrolysis process has been proven to improve the pyrolysis efficiency and the hydrogen production rate [62]. Xiao et al. developed a two-stage fixed bed system for plastic plasma-catalytic pyrolysis [35]. Compared with conventional two-stage fixed bed catalytic pyrolysis, single plasma process, and single catalysis process, the plasma-catalytic pyrolysis of PP achieves an increased gas product of 47 wt% with a much higher hydrogen yield of 4.19 mmol g_{PP}^{-1}. Also, the plasma-catalytic pyrolysis process shows an improved selectivity towards benzene, xylene, and toluene, and reduced production of wax. In plasma-catalytic pyrolysis, plasma can enhance the pre-cracking of heavy intermediates into light intermediates which could enter catalysts' inner pores/sites. In addition, plasma treatment can upgrade the catalytic performance by contributing to the formation of acid sites and defects on the catalyst surface (Fig. 4). Thus, plasma-catalytic pyrolysis shows promising potential for meeting

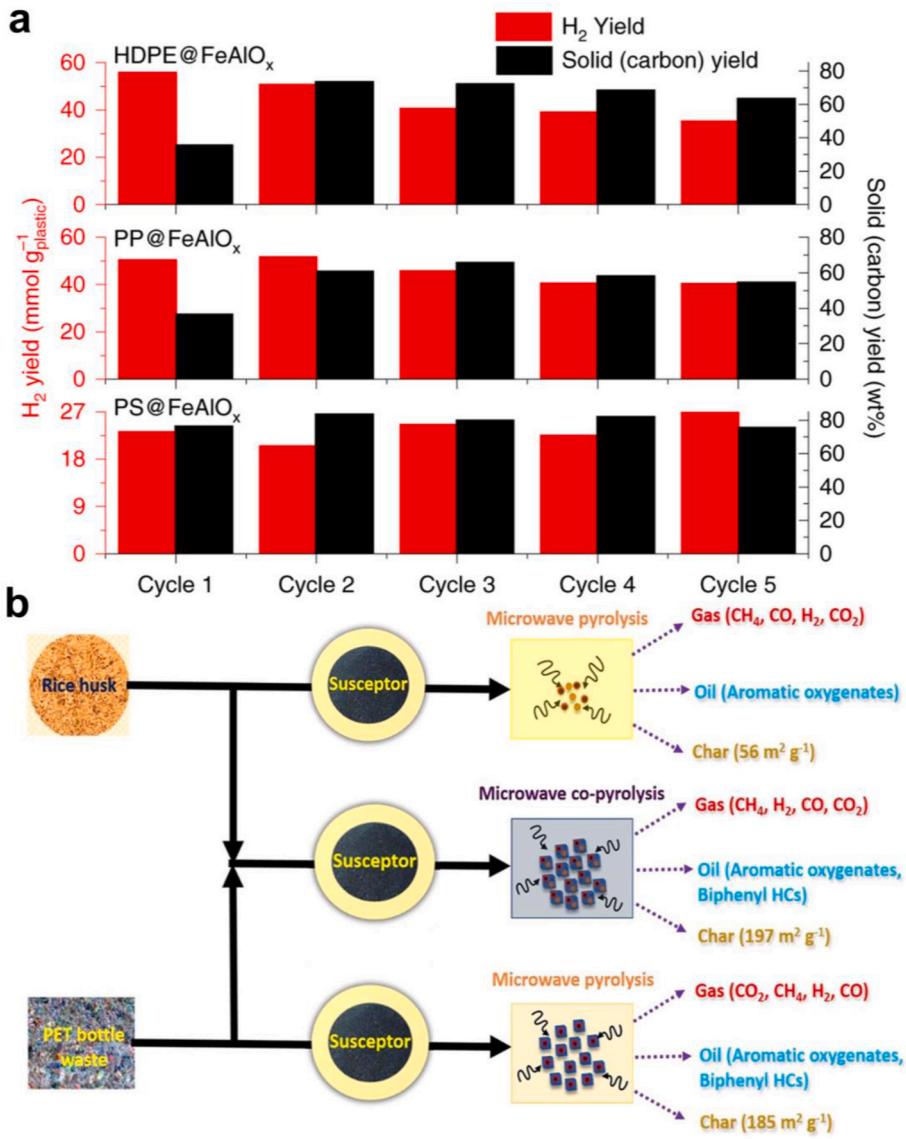

Fig. 6. (a) Successive cycles of microwave pyrolysis of HDPE, PP, and PS over $FeAlO_x$ catalyst (HDPE: high density polyethylene, PP: polypropylene, PS: polystyrene). Reproduced with permission from Ref. [66] Copyright 2020 Springer Nature. (b) Scheme of the microwave co-pyrolysis of PET and rice husk (PET: polyethylene terephthalate, HCs: hydrocarbons). Reproduced with permission from Ref. [74] Copyright 2022 Elsevier.

the challenges of low product quality and catalyst deactivation in plastic-to-hydrogen conversion. Considering the advantages of fluidized bed/spouted bed reactors in enhancing pyrolysis efficiency, it is suggested to incorporate plasma treatment into the two-stage fluidized bed/spouted bed-involved systems.

2.1.3. *Microwave pyrolysis*

Heating is the major cost of plastic pyrolysis. Conventional pyrolysis methods lead to huge costs because of the low heating efficiency and prominent heat/energy loss. Accordingly, recent attempts have utilized microwave heating to treat plastic wastes [63]. Different from the conventional heating methods with electrical heaters or burners, microwave irradiation can penetrate plastics' inside section and heat the solid homogeneously via molecular interaction with the electromagnetic field [64]. As a result, microwave pyrolysis can provide rapid heating, short reaction time, and low energy loss [65]. Recently, some interesting studies have focused on microwave-assisted plastic-to-hydrogen conversion [37]. Jie et al. have studied microwave and conventional thermal processes for HDPE conversion in terms of product composition and hydrogen yield [66]. Compared to conventional thermal pyrolysis, microwave pyrolysis can attain a higher ratio of gas products and a higher hydrogen yield (Fig. 5a). Similar results were reported by Wang and coworkers, who found a higher hydrogen yield (50.2 vs. ~ 25 mmol H_2 g^{-1}_{HDPE}) and a higher selectivity towards hydrogen (91.5 vol% vs. ~ 66 vol%) of microwave pyrolysis over the conventional thermal process in the treatment of HDPE (Fig. 5b) [37].

The hydrogen production of microwave pyrolysis processes is significantly influenced by the catalyst (microwave absorbents), process parameters, and plastic feedstock. As depicted in Fig. 5b, the catalysts composed of Ni nanoparticles-CeO_2 with a carbon nanotube (CNT) substrate (Ni–CeO_2@CNTs) show much better performance for hydrogen production compared to bare CNT, and the optimal $Ni_{1.25}Ce_{0.5}$ catalyst can gain a high H_2 selectivity (91.5 vol%) and a high H_2 yield of 50.2H_2 g^{-1}_{HDPE} [37]. Several studies have implemented $FeAlO_x$ as the catalyst for microwave pyrolysis [36,66,67]. In the microwave pyrolysis of HDPE, $FeAlO_x$ performs better than a group of metal and carbon-based catalysts (i.e., Fe, Fe_2O_3, Fe_3O_4, Fe_3C, Ni, Co, Co_3O_4, Fe/SiC, Fe/Al_2O_3, Fe/ZSM-5, Fe/activated carbon, graphite, activated carbon) with a much higher hydrogen yield of over 55.6 mmol $g^{-1}_{plastic}$ [66]. Wang et al. found that the $FeAlO_x$ catalyst can attain a high

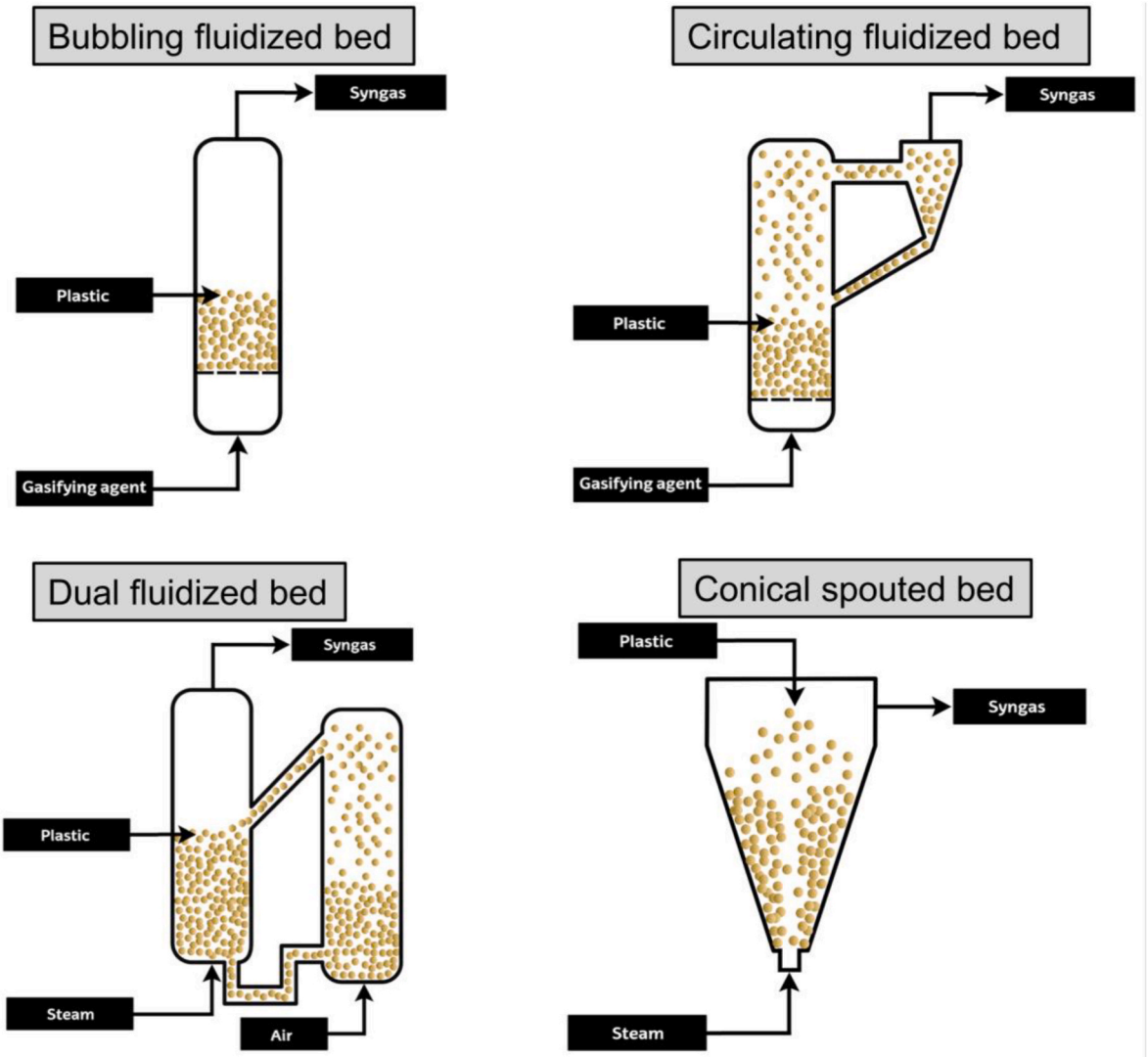

Fig. 7. Representative fluidized bed reactors and spouted bed reactors for plastic gasification. Reproduced with permission from Ref. [76] Copyright 2018 Elsevier.

hydrogen concentration (67.85 vol%) and a high hydrogen yield (48.1 mmol $g_{plastic}^{-1}$) in the microwave pyrolysis of PE, with the starting weight ratio of PE to $FeAlO_x$ at 1:1 [36]. In addition, a CNTs@Fe_3O_4/Fe_3C/Fe composite with excellent microwave absorption properties is generated during the pyrolysis process.

To regulate the composition of gas products from microwave pyrolysis, a post-catalysis process has been integrated with microwave pyrolysis [68]. Based on the microwave pyrolysis-*ex-situ* catalytic upgrading technique, Fan et al. further developed a two-stage continuous-stirred microwave pyrolysis (CSMP)- *ex-situ* catalysis process [69]. The stirring unit can enhance the mass transfer and accelerate the pyrolysis process. Compared with single microwave pyrolysis of linear LDPE, the two-step catalytic continuous pyrolysis process generates a higher hydrogen ratio in the gas product. In addition, the CSMP needs a significantly lower energy requirement than the batch microwave pyrolysis (12.83 vs. 77.42 MJ kg^{-1}), suggesting a much cleaner process for plastic-to-hydrogen upcycling. Some process parameters have been discussed in the optimization of plastic microwave pyrolysis. The hydrogen volume yield shows a positive relationship with the catalyst loading increased from 0 to 20%, while the feeding rate has little effect on hydrogen production [70]. Generally, a higher pyrolysis temperature (microwave power) and catalysis temperature, a higher hydrogen yield. The main reason should be the higher pyrolysis temperature favors the chain scission of hydrocarbons with diverse chain lengths and improved aromatization [68,71]. Different plastic feedstocks lead to distinct hydrogen production rates. For example, the average hydrogen yields of five successive pyrolysis cycles are ~50 mmol g_{HDPE}^{-1}, ~42 mmol g_{PP}^{-1}, and ~24 mmol g_{PS}^{-1} respectively, in the presence of $FeAlO_x$ catalyst (Fig. 6a) [66]. Co-pyrolysis of plastics with biowastes has also been investigated [72–74]. Although these studies do not focus on plastic-to-hydrogen conversion, the interaction between plastics and biowastes in the pyrolysis process has been evidenced and has shown profound effects on product selectivity (Fig. 6b) [74]. With the co-pyrolysis platform, further work is suggested to take advantage of the plastics-biowastes interaction for enhancing hydrogen production.

2.2. Gasification

In the gasification process, plastics can react with gasifying agents (e.g., steam, oxygen and air) at high temperatures around 500–1300 °C, which generally produces syngas [75]. A main advantage of gasification compared to pyrolysis is the greater flexibility to jointly valorize plastics of different compositions or mixtures or plastics mixed with other feedstocks [76]. The sticky behavior, high volatile content, and low thermal conductivity of plastic wastes lead to great challenges in conventional gasification techniques [76]. To this end, designing proper gasifiers is of vital importance, and some features should be met for a desirable gasifier: (i) provide high heat transfer efficiencies to realize

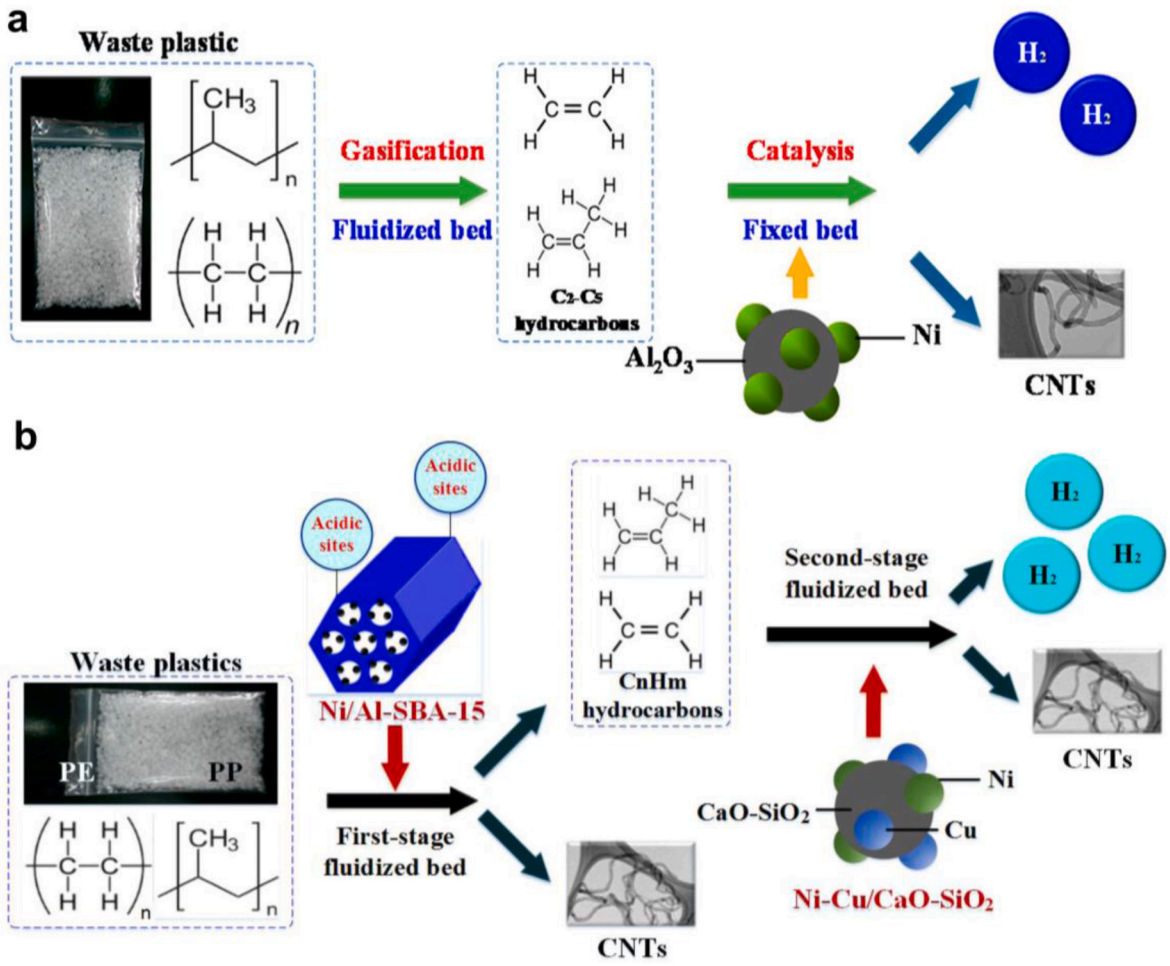

Fig. 8. (a) Scheme of the fluidized bed air-gasification-fixed bed catalysis for plastics upcycling. Reproduced with permission from Ref. [83] Copyright 2018 American Chemical Society. (b) Illustration of plastics gasification in a two-stage fluidized catalytic bed system (CNTs: carbon nanotubes). Reproduced with permission from Ref. [38] Copyright 2020 Elsevier.

fast plastics de-polymerization processes, (ii) suitable residence time distribution to facilitate the tar cracking, and (iii) have good management of operating conditions to address plastics' sticky nature. Currently, some sophisticated gasifiers have been developed, such as fluidized bed reactors and spouted beds, as shown in Fig. 7 [76]. These advanced reactors have significantly improved the plastic gasification process, compared to conventional fixed bed systems. Aside from the two-stage pyrolysis-gasification technique discussed in Section 2.1.1, this part mainly focuses on advanced gasification processes for plastics-to-hydrogen conversion.

2.2.1. *Air gasification*

Using air as the gasifying agent, air gasification holds the merit of a simplified gasification process and reduced operating/maintenance cost [82]. This process has been widely used for plastic waste upcycling, in most cases, fluidized beds with diverse variations are implemented. Overall, the hydrogen production efficiency is largely determined by the gasifier, equivalence ratio (ER), reaction temperature, bed materials, etc. Hence, in this part, the development of advanced air gasifiers and the optimization of process parameters are analyzed.

Single-stage fluidized bed gasifiers are the simplest device for air gasification. Previous studies have investigated the effect of ER, bed materials, air composition, and reaction temperature on the properties of gas products. Zhao et al. have explored the influence of oxygen proportion in the gasification stream on the production of hydrogen. Increasing the oxygen concentration from 21% to 35%, an improvement of the hydrogen ratio in gas products (3.4 vol% to 4.95 vol%) is observed [77]. Thus, an oxygen-enriched air fluidized bed might benefit the selective production of hydrogen. Similar results were also reported by Mastellone and co-authors, who verified that a higher oxygen concentration led to a better hydrogen ratio in syngas products due to improved bed temperature, in a bubbling fluidized gasifier [78]. Bed materials play a vital role in regulating gas products. Toledo et al. found that increased olivine in the gasifier bed contributed to more hydrogen production from 4 vol% to 10 vol% [79], which is mainly because of olivine's catalytic effect [80]. ER is another important factor, which can change the bed temperature and tar cracking temperature. Generally, a higher ER in a certain range leads to a higher bed temperature and a higher cracking temperature, thereby benefiting the decomposition of plastics (initial pyrolysis, tar cracking, and char gasification) and the formation of hydrogen gas [81,82].

A two-stage air gasification-catalysis process has been developed for the production of hydrogen and CNTs from plastics. As illustrated in Fig. 8a, the gasification-catalysis process consists of a fluidized gasifier and a subsequent catalytic fixed bed [83]. In this process, raising the reaction temperature and decreasing the ER can enhance the methane and hydrocarbon dry reforming and hydrocarbon direct decomposition for the co-production of hydrogen fuel and CNTs. Under the optimal conditions, a hydrogen production rate of 385.1 mmol h^{-1} g_{cat}^{-1} can be achieved, using a Ni/Al_2O_3 catalyst. The catalyst properties can impact the hydrogen production rate by regulating the dry reforming of methane and hydrocarbons [84]. Compared with samples treated in air

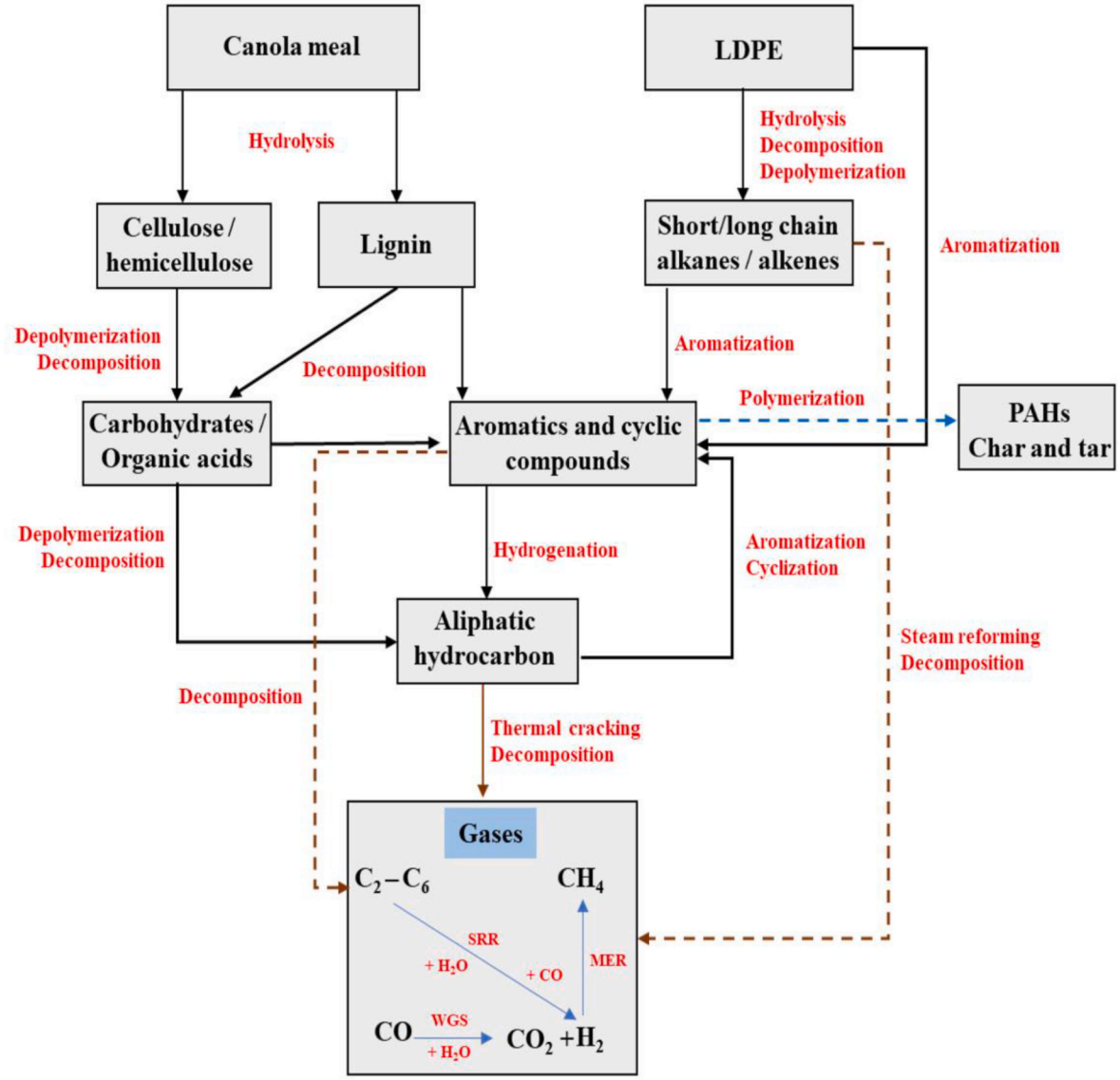

Fig. 9. Reaction mechanisms for co-gasification of LDPE and canola meal (LDPE: low density polyethylene, PAHs: polycyclic aromatic hydrocarbons, SRR: steam reforming reaction, MER: methanation reaction). Reproduced with permission from Ref. [111] Copyright 2022 Elsevier.

and N_2 atmosphere, the Ni/Al_2O_3 catalyst calcined under the 5% H_2/He condition shows optimal catalytic performance for hydrogen production owing to its smallest Ni crystallite and enhanced metal dispersion [85]. A further breakthrough in the gasification process design is the two-stage fluidized-bed reactor system, as shown in Fig. 8b [38]. Ni/Al-SBA-15 and Ni–Cu/CaO–SiO_2 catalysts are used for CNTs and hydrogen production in the first and second stages respectively, and the hydrogen yield reaches 857.6 mmol h^{-1} g_{cat}^{-1}.

Combining the fluidized bed gasifier with a tar-cracking reactor can limit the production of tar, and the developed two-stage gasification reactor is called the University of Seoul (UOS) gasifier [86]. A main feature of the UOS gasifier is that it can significantly reduce the tar production in the gas product via tar-cracking reactions and improve hydrogen purity. Kim et al. have done a series of studies regarding the air gasification of diverse plastic wastes with the UOS gasifier [87–94]. They have developed a series of fluidized bed materials (e.g., quicklime, dolomite, olivine, and oyster shells) and tar-cracking reactor additives (e.g., activated carbon, Ni-loaded activated carbon). In their latest study, they studied the gasification behavior of ten different types of plastics with the UOS process [93]. According to their results, activated carbon can lower the tar ratio in gas products and strengthen hydrogen production. Additionally, the air gasification of aliphatic plastics without heteroatoms (e.g., PP, PE) favors hydrogen generation and a high value of 26 vol% can be obtained.

2.2.2. *Steam gasification*

With the gasifying agent being steam, steam gasification of plastics can produce hydrogen-rich syngas with a high H_2/CO ratio [95]. The central challenge of steam gasification is efficient heat input into the reactor for endothermic steam reforming reactions [76]. Thus, much work has been done in designing practical steam gasifiers for plastic conversion, and fixed beds, fluidized beds, and conical spouted beds with diverse combinations are widely investigated.

Semi-batch reactors with simple components have been used for plastic steam gasification. Kamo et al. have developed a semi-batch gasification reactor to convert PVC wastes into hydrogen gas at 3 MPa and 560–660 °C, and they found that the presence of alkali compounds could improve the hydrogen production via the reaction: $2NaOH + C + H_2O \rightarrow 2H_2 + Na_2CO_3$ [96]. In another study, a semi-batch gasification reactor is used for organic wastes steam gasification, and the co-gasification of biomass and plastics produces three times more hydrogen than mono-feedstock gasification. The reason is that the

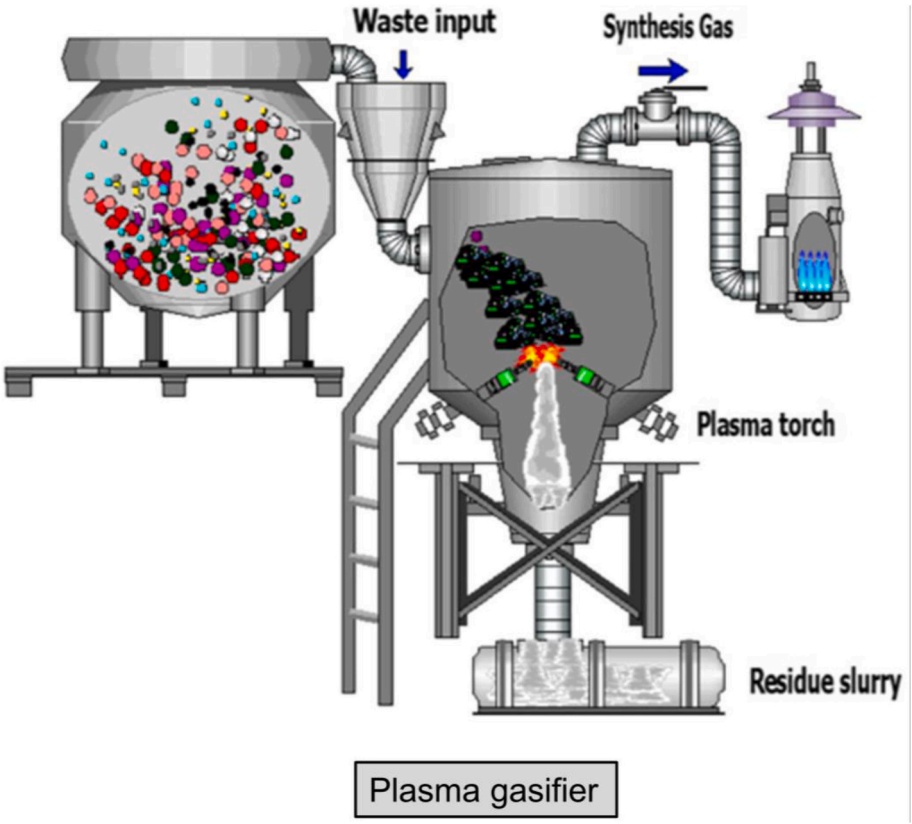

Fig. 10. Schematic diagram of the plasma gasifier. Reproduced with permission from Ref. [120] Copyright 2022 Springer Nature.

presence of use of biomass can improve the generation of lighter hydrocarbons by radical-enhanced cracking reactions [97]. The effect of plastic feeding on hydrogen production was also verified by Lopez et al. who studied the steam gasification of biomass/plastic mixture with a one-stage conical spouted bed gasifier [98]. Compared with biomass/HDPE mixture and sole biomass, the gasification of pure HDPE can attain the highest gas yield (~3.2 $Nm^3\ kg^{-1}$) and hydrogen content (~57 vol%). Thus, plastic co-feeding can improve biomass steam gasification in terms of producing hydrogen-rich syngas [99]. Catalysts are essential for enhancing hydrogen production in the steam gasification process. In the gasification of MSW with a fluidized bed reactor, the addition of CaO increases the dry gas yield and hydrogen yield. It is suggested that CaO can destabilize the aromatic rings of tar compounds and accelerate organic ring splitting, and also act as the CO_2 sorbent to decrease the concentration of CO_2 in gas products. At 900 °C, the maximum hydrogen yield reaches 104 mol kg_{MPW}^{-1} [40]. The catalytic effect also has been reported in the steam gasification of phenolic boards, in which Ni powders could enhance hydrogen formation [100].

The two-stage steam gasification-reforming process has been developed to valorize plastics. Lopez and co-authors found that the reforming temperature has a prominent on the product yield and gas composition, and a higher reforming temperature (700 °C) contributes to a higher hydrogen yield (36 wt% by a mass unit of feed HDPE) [101]. Similarly, in the dual fluidized bed steam gasification process, hydrogen production is positively correlated with gasification temperature [102]. Besides temperature, the plastic feedstock is also concerned. The combination of PE/PS is better than PE/PP, PE/PET, PP, and PE regarding a higher hydrogen concentration (>50 vol%) in dry gas products [102]. Farooq et al. [103] and Wang et al. [39] have utilized some catalysts to improve hydrogen yields. Especially, Ni-based catalysts like NiO/dolomite [39] and $Ni/CeO_2–ZrO_2$ [103] exhibit efficient catalytic performance in accelerating the water gas shift (WGS) reaction and eliminating the tar, thereby resulting in high hydrogen production.

2.2.3. Supercritical water gasification

Supercritical water gasification (SCWG) is an effective and clean method for plastic conversion. Supercritical water (SCW; T > 374 °C, P > 22.1 MPa) shows a significantly lower density, dielectric constant, and viscosity, as well as fewer hydrogen bonds [104,105]. In supercritical water, water acts as a non-polar solvent which can solve the problems of poor heat transfer and high viscosity by dissolving the plastic fragments [106]. Moreover, water also acts as a hydrogen donor which helps plastic cracking and gasification. Accordingly, the resistance among different phases is significantly limited, thus accelerating gasification processes [41]. The plastic SCWG is generally implemented in a batch reactor, which is made of quartz or superalloy and can withstand high temperatures and pressures [43,107].

SCWG has been used to treat diverse waste plastics, and the reaction temperature, time, catalysts, water/plastic ratio, and plastic type are important factors that influence hydrogen production performance. Generally, a higher temperature can accelerate the endothermic steam reforming and decomposition reactions and thus result in higher hydrogen yields [39,43,108]. In the SCWG of lignite/PP mixtures, the hydrogen yield increases from ~1 mol kg^{-1} to 24.17 mol kg^{-1}, with the reaction temperature from 500 °C to 800 °C [41]. Hydrogen yields increase with reaction time, which is contributed by the gradual increase in gas products and hydrogen fraction. With increasing reaction time, steam reforming reactions will continue to happen, leading to improved gasification efficiency and more gas products [109]. The water/plastic ratio (feedstock concentration) has been investigated in the SCWG process, and some studies suggest that a higher water/plastic ratio favors hydrogen production [41,42,106,110]. When a high plastic concentration is used, the low water proportion could not enable a complete SCWG reaction, resulting in a lower hydrogen fraction in gas products [42]. In addition, the decline in the water ratio can limit the hydrocarbon reforming reaction, in turn decreasing the hydrogen fraction in gas products [41]. The presence of catalysts can improve hydrogen yield

Table 2
Representative achievements in photocatalytic upcycling of plastics for hydrogen fuel (PS: polystyrene; PE: polyethylene; PET: polyethylene terephthalate; PLA: polylactic acid).

Photocatalyst/ Electrocatalyst	Plastic	Reaction conditions	Hydrogen production performance
MoS_2/CdS [123]	PE	10 M KOH solution; Light source: 300 W Xe lamp; T: 5 °C	H_2 yield: 1.13 ± 0.06 mmol g^{-1} h^{-1}
CdS/MoS_2 [124]	PLA	10 M KOH solution; Light source: 300 W Xe lamp	H_2 yield: 379.5 mmol g^{-1} h^{-1}
MXene/$Zn_{0.6}Cd_{0.4}S$ [125]	PET	10 M KOH solution; Light source: 300 W Xe lamp	H_2 yield: 14.17 mmol g^{-1} h^{-1}
CdS/CdO_x [126]	PLA	10 M KOH solution; Light source: 300 W Xe lamp	H_2 yield: 64.3 ± 14.7 mmol g_{CdS}^{-1} h^{-1}
Pt 0.5 wt%-deposited CdO_x/CdS/SiC [127]	PE	10 M NaOH solution; Light source: 300 W Xe lamp; T: 70 °C	H_2 yield: 25 μmol g^{-1} h^{-1}
Pt 0.5 wt%-deposited CdO_x/CdS/SiC [127]	PS	10 M NaOH solution; Light source: 300 W Xe lamp; T: 70 °C	H_2 yield: 19.4 μmol g^{-1} h^{-1}
Carbonized polymer dots-graphitic carbon nitride [128]	PET	1 M KOH solution; Light source: 300 W Xe lamp; T: 40 °C	H_2 yield: 1034 ± 134 μmol g^{-1} h^{-1}
Benzenesulfonyl chloride-incorporated g-C_3N_4 [129]	PLA	1 M KOH solution; Light source: 300 W Xe lamp; T: 10 °C	H_2 yield: 1890 μmol g^{-1} h^{-1}
$Ni_xCo_{1-x}P$/reduced graphene oxide/g-C_3N_4 [130]	PLA	1 M KOH solution; Light source: 300 W Xe lamp; T: 10 °C	H_2 yield: 576.7 μmol m^{-2} h^{-1}
Ag_2O/Fe-MOF [131]	PET	Deionized water; Light source: 300 W Xe lamp; T: 25 °C	H_2 yield: 1.9 mmol g^{-1} h^{-1}
α-Fe_2O_3/polypyrrole [132]	PLA	10 M NaOH solution; Light source: visible light household lamp (5 W cm^{-2})	H_2 yield: 78.6 mmol g^{-1} h^{-1}
CN-CNTs-NiMo hybrid [133]	PET	5 M KOH solution; Light source: 500 W Xe lamp; T: 15 °C	H_2 yield: 90 μmol g^{-1} h^{-1}

and plastic gasification efficiency [111]. A recent machine learning study has compared different alkali catalysts and transition metal catalysts in the plastic SCWG. Among different catalysts, K_2CO_3 is the best alkali catalyst under optimal process conditions, with a maximum hydrogen yield of 76.78 mol kg^{-1}. For transition metal catalysts, Fe-based catalysts exhibit better performance than Ru, Ti, Ni, Zn, Cu, and Co-based counterparts in SCWG [112].

Different plastic feedstocks for SCWG result in distinct hydrogen yields. Onwudili and co-authors found that the SCWG of PS could produce more hydrogen gas than PP, HDPE, and LDPE [110]. However, the hydrogen gasification efficiencies (HGE) and carbon gasification efficiencies (CGE) of PS are the lowest, and the reason remains unclear. Considering the efficient SCWG process for handling organic wastes, some studies have investigated the co-gasification of plastics and biowastes. In the SCWG of food waste with various ratios of plastics, a lower plastic content in food waste favors hydrogen production and contributes to a higher gasification efficiency [108]. Cao et al. found a synergetic effect in the co-gasification of soda lignin and PE, with the optimal performance obtained at the mix ratio of 1:1. A possible reason is that the alkali salts in soda lignin can act as effective catalysts in SCWG of plastics for enhancing hydrogen generation [43]. Nanda et al. also proposed a synergetic effect in the hydrothermal co-gasification of LDPE and canola meal [111]. As depicted in Fig. 9, the decomposition of LDPE and canola meal gives rise to the formation of a series of intermediates, and two main reaction mechanisms (e.g., ionic and free radical mechanisms) can work together to convert different reactants and promote hydrogen production.

2.2.4. Plasma gasification

Plasma gasification is an eco-friendly technique for converting plastics into valuable syngas. Plasma gasification is an allothermal process i.e., the electrical energy is supplied externally through a plasma torch which raises the gasifier to a very high temperature (over 1500 °C) depending on the torch power. Plasma gas in the reaction works as a reforming agent that breaks plastics in the gas phase into lighter molecules [113]. The temperature inside the plasma zone varies in a wide range, and it can be up to 14000 °C, thus enabling a fast gasification process [31]. The plasma gasifier is simple, as shown in Fig. 10, and hydrogen production is influenced by the input power, plasma gas, plastic feedstock, etc. In the plasma gasification of wood sawdust and HDPE mixtures, the yield and proportion of H_2 show a climbing trend with the increase of input power, while exhibiting a trend from rising to descending with the increase of steam flow/carbon flow ratio [45]. In the gasification of plastic and MSW mixtures, adding steam to the plasma gas produces a high hydrogen concentration in the syngas [114]. Yun et al. also suggested that an increased steam/fuel ratio promoted WGS and ion-reforming reactions, thereby favoring hydrogen production from glass fiber-reinforced plastic (GFRP) in a microwave plasma reactor [115]. In addition, a high plastic/MSW ratio promotes the hydrogen mole fraction due to the higher hydrogen content in plastics. Hlina et al. found that the high temperature and low mass flow rate benefited the generation of syngas with a high hydrogen ratio [116]. However, the required high electricity demand would limit the large-scale application of the high-temperature process. Alternatively, Tabu and coworkers have developed two nonthermal atmospheric plasma reactors based on the transferred arc and gliding arc discharges for LDPE upcycling [44]. In both reactors, hydrogen yields increase with the voltage level, and the optimal hydrogen yields for gliding arc and transferred arc reactors reach 0.42 and 0.33 mmol g_{LDPE}^{-1}, respectively.

Two-stage processes based on plasma gasification gain growing interest. Sikarwar and co-authors have designed a plasma gasification-CO_2 sorption-enhanced reforming technique to treat a mixture of plastics and biowastes. Compared with the single plasma gasification process, the implementation of a post-reforming unit largely benefits the production of hydrogen-rich syngas. In the reforming process, the performance of CaO sorbent is better than MgO and Li_4SiO_4, and a higher temperature benefits hydrogen production [117]. Integrating gasification with a plasma reforming unit is efficient for enhancing syngas production in HDPE gasification. The thermal plasma can enhance hydrogen production by hydrocarbon reforming and cracking [118]. The enhancement was also reported by Nguyen et al. who employed a non-thermal plasma reforming process to regulate the syngas composition produced from the thermal treatment of HDPE [119]. In the non-thermal plasma process, the hollow structural ZSM-5 catalyst delivers better hydrocarbon deconstruction performance than the nanoparticle counterpart, showing the critical role of catalyst properties in thermochemical reactions.

3. Photo-reforming

Photo-reforming or photocatalysis of plastics emerges as a relatively cheap and green technique because of its mild reaction requirements of ambient temperature and pressure and using sustainable solar energy as the energy source [19]. Additionally, the mild photocatalytic process shows high potential for the precise activation/break of typical chemical bonds in plastic polymers, which helps realize the selective production of targeted value-added chemicals [121,122]. Using efficient semiconductor photocatalysts, the photo-reforming of plastic wastes has successfully converted plastics into hydrogen fuel and small molecule organic chemicals or CO_2/H_2O, as shown in Table 2.

3.1. Mechanism of plastic waste photo-reforming

The plastic photo-reforming process generally contains three elemental steps: (1) the absorption of photons by photocatalysts and the

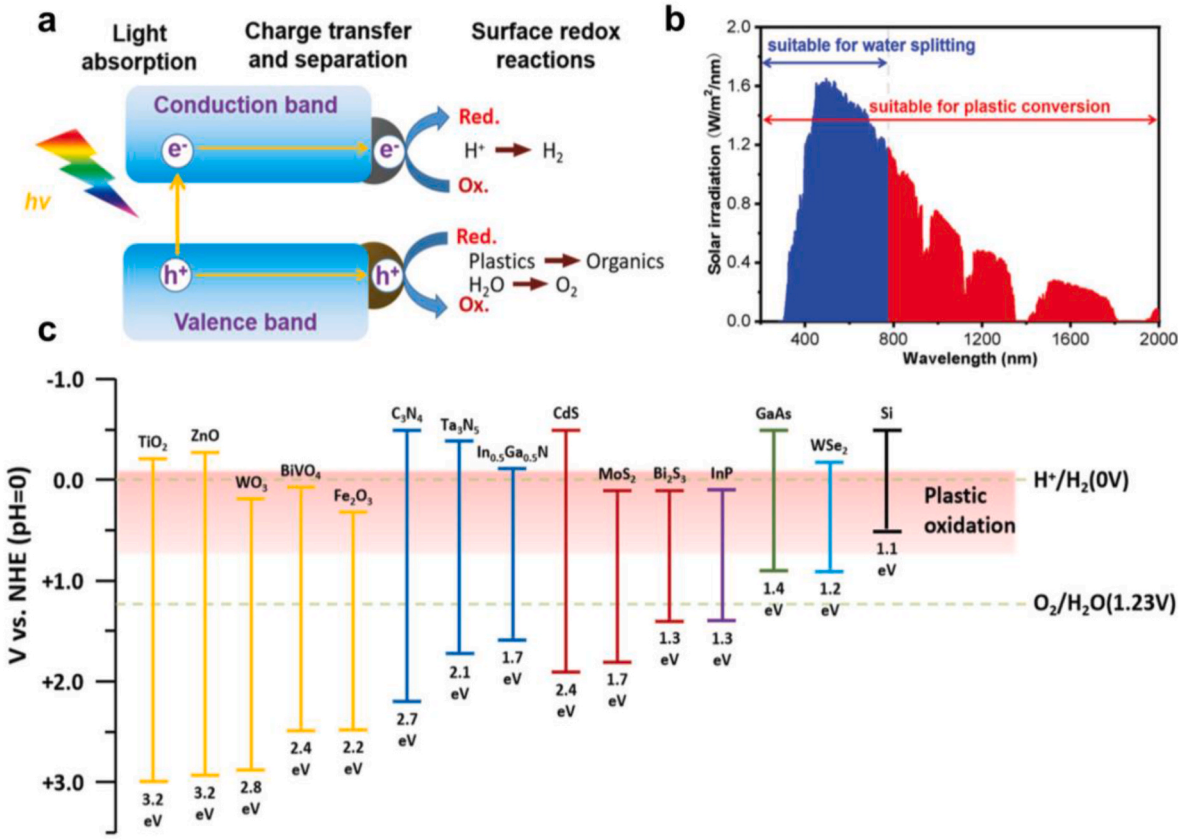

Fig. 11. (a) Scheme of the three-step process of plastic photo-reforming. (b) The global standard solar spectrum (AM 1.5G) and sections of sunlight suitable for plastic conversion and photocatalytic water electrolysis. (c) Band edge positions and bandgaps of representative semiconductor photocatalysts (NHE: normal hydrogen electrode). Reproduced with permission from Ref. [136] Copyright 2022 Wiley-VCH.

excitation of electron-hole pairs, (2) the separation and migration of photogenerated charge carriers, and (3) photogenerated holes and electrons-triggered surface redox reactions (Fig. 11a). The photogenerated holes can oxidize plastics and the photogenerated electrons can reduce water to produce hydrogen fuel. Compared to conventional photocatalytic water splitting which consists of water oxidation and proton reduction, plastic photocatalytic upcycling is a more efficient process. Generally, high energy (>1.6 eV) is necessitated to initiate the photocatalytic water splitting, due to the reaction kinetic hindrance, especially for the sluggish 4-electron OER [134,135]. However, only 43% of available solar photons possess energy over 1.6 eV, and a large proportion of solar energy cannot be used. Alternatively, plastic oxidation is a more efficient process because of its lower energy barrier, thereby decreasing the required energy to couple with hydrogen production. Plastic photo-conversion represents a less energetically demanding process than photocatalytic water splitting, and a larger portion of the solar spectrum can be utilized for plastic photo-reforming (Fig. 11b) [136].

In plastic photo-conversion, plastics show a similar role as sacrificial agents in traditional photocatalysis systems, which are fully or partially oxidized by photogenerated holes. Compared to conventional expensive sacrificial reagents (e.g., triethylamine, methanol), using plastic polymers as hole scavengers to improve hydrogen production can co-generate value-added chemicals at low cost.

3.2. Advanced photocatalysts

As shown in Fig. 11c, plastic photo-oxidation can be achieved by narrower bandgap photocatalysts. Compared with metal oxides with deep valance bands, metal phosphides, selenides, nitrides, arsenides, sulfides, and silicon show insufficient photooxidation potentials for OER, but they are capable of oxidizing plastic wastes. Currently, a series of high-performance composite photocatalysts have been developed for plastic photo-reforming.

CdS-based composites. With a wide bandgap of ~2.4 eV and suitable band positions (conduction band (CB): 0.5 V vs. NHE, valence band (VB): + 1.9 V vs. NHE), CdS is capable of visible light absorption and is in favor of photocatalytic redox reactions. Nevertheless, the photocorrosion, rapid recombination of photogenerated electron-hole pairs, and insufficient photoactive sites of CdS limit its photocatalytic applications. Constructing composite catalysts is a sophisticated method to address these issues. For example, Du et al. developed a MoS_2/CdS hybrid for the photo-reforming of pretreated PE, PET, and PLA. Taking advantage of the anisotropic morphology and the rapid/facile charge transfer feature of the nanorod structure, the MoS_2/CdS composite can collect electrons at the MoS_2 tip toward water reduction to hydrogen and utilize the sidewall of the CdS nanorod with rich holes for plastic photooxidation (Fig. 12a) [123]. Compared with PET and PE, the photo-conversion of PLA can attain a higher hydrogen production rate and higher oxidation selectivity. Similar results were also obtained from a study by Zhao et al. in which a CdS/MoS_2 nanooctahedrons composite was designed for the photochemical plastic-to-hydrogen conversion [124]. MXene has high electrical conductivity and a favorable Fermi level position, which makes it an effective catalyst promoter to upgrade electron-hole pairs separation, enhancing the photocatalytic activity of CdS. The MXene/$Zn_xCd_{1-x}S$ composite photocatalysts show a better activity for PET reforming than the single components, and the hydrogen production is highly component-dependent (Fig. 12b) [125]. Fig. 12c further discloses the catalytic mechanism that the holes in the VB of $Z_xC_{1-x}S$ act as the active species for PET oxidation, and the electrons in MXene transferred from the CB of $Z_xC_{1-x}S$ can reduce water to hydrogen. CdS/CdO_x composites also show promising performance for plastic

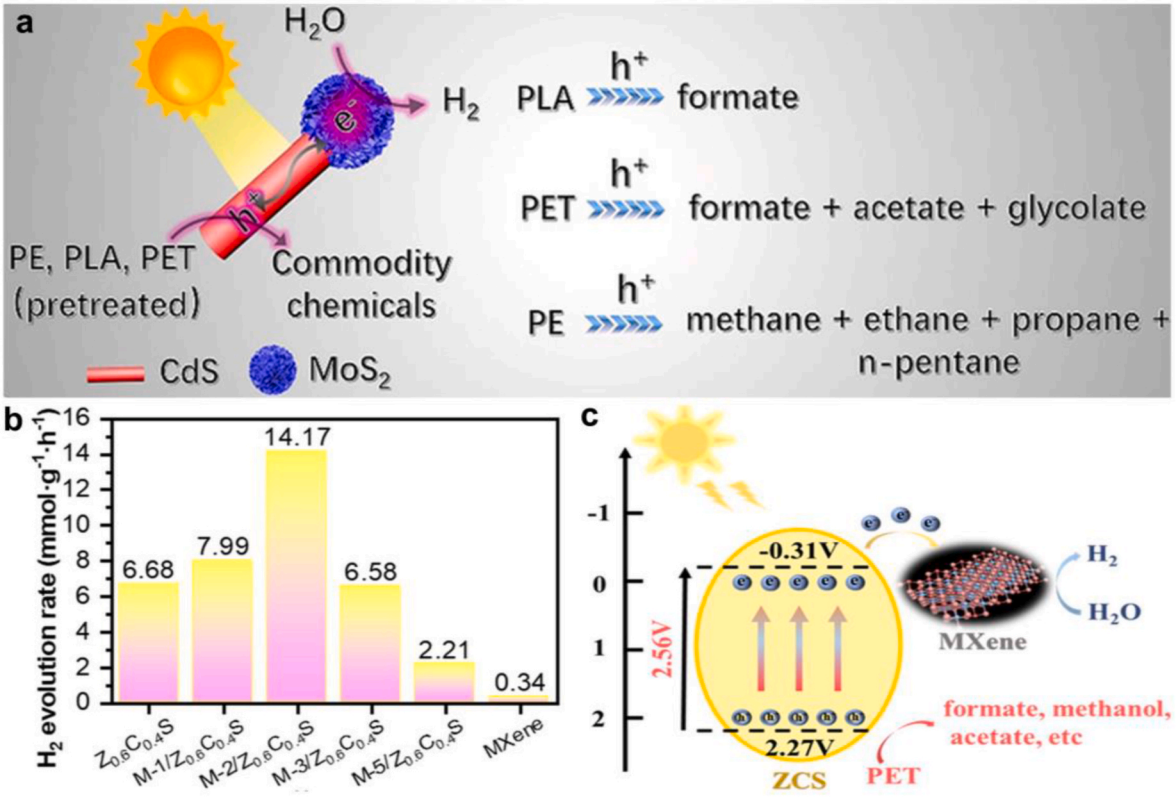

Fig. 12. (a) Scheme of pretreated plastics photo-reforming over CdS/MoS_2 photocatalyst (PLA: polylactic acid, PET: polyethylene terephthalate, PE: polyethylene). Reproduced with permission from Ref. [123] Copyright 2022 American Chemical Society. (b) Photocatalytic H_2 evolution with MXene/$Z_xC_{1-x}S$ catalysts. (c) Illustration of PET photo-reforming mechanism over the M−2/$Z_{0.6}C_{0.4}S$ catalyst (ZCS: $Z_{0.6}C_{0.4}S$). Reproduced with permission from Ref. [125] Copyright 2022 Elsevier.

upcycling. The CdS/CdO_x quantum dots developed by Uekert and co-authors realize the efficient photo-reforming of PLA, PET, and polyurethane (PUR) [126]. More recently, a $CdO_x/CdS/SiC$ composite has been reported for organic waste photocatalytic conversion. The $CdO_x/CdS/SiC$ catalyst has wide absorption for visible and ultraviolet lights, and the excellent thermal radiative ability can help increase the temperature of the reaction system and promote organic waste hydrolysis. During the photocatalysis process, CdS forms a stable and very thin oxide film in the alkaline solution and the water reduction proceeds, leading to hydrogen generation on the CdS side. With the deposited Pt co-catalyst, electrons could transport to Pt and a hydrogen evolution reaction happens on the Pt surface [127]. Among the cellulosic biomass, plastics, and protein substrates, the hydrogen production amount from plastics is the lowest.

Carbon nitride-based composites. Carbon nitride (CN) is a promising photocatalyst due to its appropriate electronic band structure, facile synthesis, non-toxicity, high chemical stability, and low cost [137,138]. The photocatalytic performance of bulk CN is severely hindered by its rapid recombination of photogenerated photo-generated charge carriers [139]. To enhance its performance, many CN-based composites have been developed for plastic upcycling. Using carbonized polymer dots-graphitic CN hybrid (CPDs-CN) as the catalyst, the photo-reforming of PET can lead to high-purity monomer terephthalic acid from PET oxidation and a high hydrogen yield of 1034 ± 134 μmol g^{-1} h^{-1} [128]. Another metal-free composite benzenesulfonyl chloride incorporated CN (BS–CN) has been used for PLA photo-reforming, and the intramolecular donor-acceptor conjugation in BS-CN contributes to a quick intramolecular electron transfer [129]. Compositing metal phosphides with CN also has been reported. The Ni_2P/CN catalyst has shown excellent performance toward PET and PLA photo-reforming [140,141]. It is suggested that the metallic Ni_2P can improve charge separation and photocatalysis. To further upgrade the catalytic performance of metal/CN composites, introducing highly conductive carbon materials with a large surface area has been attempted. As reported by Yan et al. the $Ni_xCo_{1-x}P$/reduced graphene oxide (rGO)/CN heterostructure attains a hydrogen production rate of 576.7 μmol h^{-1} g^{-1} for PLA reforming, which is 3.6 times over the binary $Ni_xCo_{1-x}P$/CN counterpart. Further analyses indicate that the photogenerated electrons transfer along the route of CN→rGO→$Ni_xCo_{1-x}P$, where rGO and $Ni_xCo_{1-x}P$ work as the electron transfer medium and water reduction site, respectively [130]. In a similar CN-carbon nanotubes-NiMo hybrids (CN-CNTs-NM), the strong π-π interaction between CN and CNTs accelerates electron transfer, improves carrier lifetime and thus enhances PET and PLA photo-reforming activities [133].

Metal oxide-based composites. Several metal oxides-based composites have been designed for plastic-to-hydrogen conversion. Starting from FeAg bimetallic metal-organic frameworks (MOF), Qin et al. synthesized a Ag_2O/Fe-MOF composite for microplastics conversion [131]. The band configuration of the Ag_2O/Fe-MOF heterojunction is shown in Fig. 13a, and the integration of Ag_2O and Fe-MOF leads to the formation of a p-n junction at the interface. Accordingly, the internal electric field could accelerate photogenerated carriers' transfer across the heterojunction and boost photocatalysis. The oxidation of microplastics produces value-added formic acid, and a possible reaction pathway is presented in Fig. 13b. Compared with the single Ag_2O and Fe-MOF, the composite shows a higher hydrogen production rate of 1.9 mmol g^{-1} h^{-1} and 1.7 mmol g^{-1} h^{-1} from PET and PE microplastics conversion, respectively (Fig. 13c). Recently, an iron oxide/polypyrrole composite has been developed for PLA photo-reforming, and the hydrogen production rate is 78.6 mmol g^{-1} h^{-1} at 168 h [132]. Although the inorganic/organic composite is capable of converting plastic wastes to hydrogen and value-added chemicals, the underlaying mechanism needs further exploration. Beyond harvesting hydrogen fuel from plastics, Xu and co-authors found that the application of Co–Ga_2O_3 nanosheets could

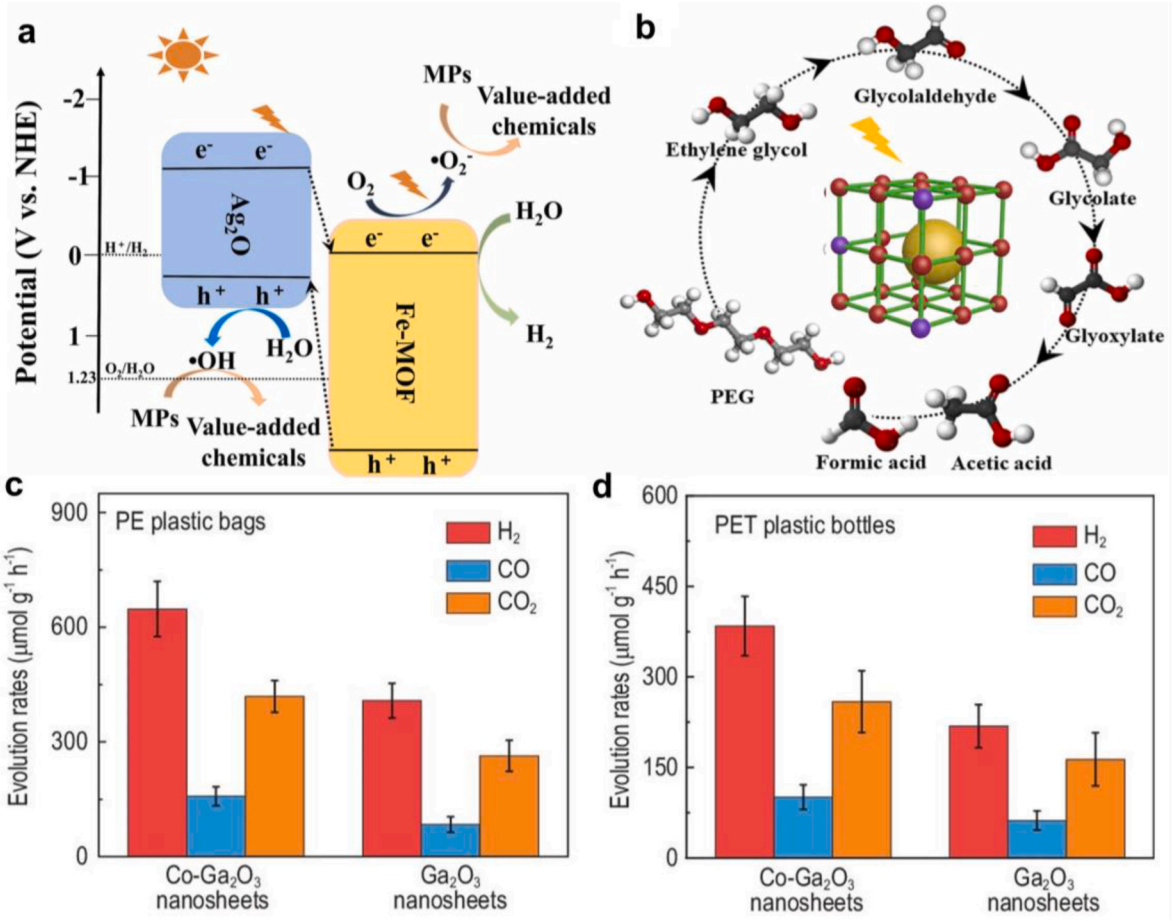

Fig. 13. (a) Plastic photo-reforming mechanism over the Ag_2O/Fe-MOF hybrid (MPs: microplastics). (b) Possible conversion pathway of PEG (PEG: polyethylene glycol). Reproduced with permission from Ref. [131] Copyright 2022 Elsevier. Photo-reforming of (c) PE plastic bags and (d) PET plastic bottles into syngas over Co–Ga_2O_3 and Ga_2O_3 catalysts (PET: polyethylene terephthalate, PE: polyethylene). Reproduced with permission from Ref. [142] Copyright 2022 Oxford University Press.

produce syngas from PE and PET (Fig. 13c and d) [142]. The H_2 and CO formation rates are related to plastics' type and catalysts' properties. The plastics-to-syngas conversion mechanism involves a three-step process: 1) H_2O is split into O_2 and H_2, 2) plastics are oxidized into CO_2 and O_2 is reduced to H_2O synchronously, and 3) CO_2 is further reduced to CO and meanwhile H_2O is oxidized to O_2.

4. Electro-reforming

The electrochemical upcycling of plastics shows the merits of mild reaction conditions, high reaction kinetics, and selectivity. Currently, plastics like PP, PET, PMMA, PVA, and PLA have been used as the anode substrates to enhance the cathode hydrogen production efficiency via electrolysis [143–147]. These practices not only realize the energy-saving hydrogen production but also transfer plastic polymers into value-added small molecular organic chemicals, such as formic acid. Several advanced electrochemical techniques and diverse low-cost electrocatalysts have been reported for the electro-reforming of plastic wastes, and some examples are provided in Table 3.

4.1. *Electro-reforming processes and mechanisms*

Plastic electro-reforming generally involves the oxidation of plastic polymers at the anode part and the hydrogen evolution reaction (HER) at the cathode part, which generates small molecular organics and hydrogen respectively (Fig. 14a) [155]. Before electrolysis, a hydrolysis step is implemented to liberate organic molecules (e.g., ethylene glycol) from solid plastics. The generated hydrogen fuel comes from water molecules, and plastics-derived organics act as an anode substrate. Since the energy barrier for organic oxidation is lower than OER in the conventional water electrolysis scheme, the coupling of plastics-derived organic oxidation with HER can realize energy-saving hydrogen production and value-added anode products [156–159].

To limit the energy cost of hydrogen production, solar energy-powered plastic electro-reforming has been proposed. As illustrated in Fig. 14b–a solar-driven "chemical factory" based on the two-electrode electrolyzer is designed to catalyze PET upgrading and HER from seawater [153]. Of note, the favorable PET lysate oxidation process (oxidation of PET monomer ethylene glycol to formic acid (HCOOH)) significantly inhibits the chlorine evolution reaction (CER) and largely widens the safe potential window for efficient hydrogen production from seawater. This process makes full use of seawater, plastic wastes, and sustainable solar energy for the production of hydrogen fuel and chemicals, which is of great environmental and economic significance for sustainable hydrogen energy.

Combining thermal pyrolysis with electrolysis, a solar thermal electrochemical process is developed for the depolymerization of plastic wastes to generate hydrogen fuel. The thermo-coupled electrochemical reactor is shown in Fig. 14c. In the reactor, the powdered mixture of PP and the alkaline electrolyte is put into the reactor, and the eutectic electrolytes of KOH/NaOH act as a reservoir of oxygen and hydrogen elements with low molten points and high conductivity. Sunlight is irradiated to a connected solar heat concentrator and PV module for generating high-temperature heat and electricity to provide energy for

Table 3
Representative achievements in electrocatalytic upcycling of plastics for hydrogen fuel (PET: polyethylene terephthalate; MEA: membrane-electrode assembly).

Electrocatalyst	Plastic	Reaction conditions	Hydrogen production performance
$CuCo_2O_4$ [148]	PET	Two-electrode MEA electrolyzer; 5.0 M KOH; flow rate: 0.1 mL min^{-1}	H_2 yield: 1.89 L (5 g PET)
Co and Cl co-doped Ni_3S_2 [149]	PET	Two-electrode MEA electrolyzer; 2.0 M KOH; Potential: 1.7 V; flow rate: 0.2 mL min^{-1}	H_2 production rate: 50.26 mmol h^{-1}
B and Co co-doped Ni_3S_2 [150]	PET	Two-electrode MEA electrolyzer; 2.0 M KOH; current density: ~0.3 A cm^{-2}; flow rate: 0.2 mL min^{-1}	H_2 production rate: 45.38 mmol h^{-1}
Pd/nickel foam [151]	PET	Two-electrode H-type electrolyzer; 10.0 M KOH; potential: 1.01 V	H_2 production rate: 0.48 mmol h^{-1}
Pd-NiTe [152]	PET	Two-electrode H-type electrolyzer; 1.0 M KOH; potential: 2.0 V	Faradic efficiency for H_2 production: 98.6%
Ni_3N/W_5N_4 [153]	PET	Solar-powered two-electrode H-type electrolyzer; 1.0 M KOH; 1 sun illumination	Solar-to-hydrogen efficiency conversion efficiency: 16.04%
$CoNi_{0.25}P$ [154]	PET	Two-electrode MEA electrolyzer; potential: 1.7 V; 2.0 M KOH	H_2 yield: 16.9 g (1 kg PET)

the plastic upcycling process [144].

4.2. Advanced electrocatalysts

Electrocatalysts are important for enhancing hydrogen production efficiency and regulating reaction selectivity [151,160–163]. A couple of advanced electrocatalysts have been developed to replace noble metals for the electro-reforming of plastic wastes. The reaction efficiency and pathway are highly catalyst-dependent, and recent efforts mainly focus on engineering catalysts' nanostructure, composition, and electronic structures.

Earth-abundant transition metal oxide-based nanomaterials are widely studied due to their facile preparation, eco-friendliness, high electroactivity, good stability, and low cost [164–170]. For example, Wang et al. designed Cu-based nanowire catalysts for the electro-upcycling of PET hydrolysate (e.g., ethylene glycol (EG)). The electrooxidation pathway of EG on the CuO nanowire catalyst can beak the C–C bond to generate value-added formic acid with a high selectivity of 86.5% and a Faradaic efficiency (FE) of 88% [171]. However, the hydrogen production efficiency has not been analyzed. Another study reported a $CuCo_2O_4$ nanowire array catalyst for the upcycling of PET. The $CuCo_2O_4$ catalyst was prepared by a hydrothermal-annealing process (Fig. 15a), which can convert PET into formate with high selectivity and FE. Coupling with the HER process, the electro-reforming of PET plastic bottles can attain a higher current density at fixed potential compared with water electrolysis (Figs. 15b), and 1.89 L of H_2 can be obtained from 5 g of PET feedstock (Fig. 15c) [148]. Aside from electrochemical oxidation, Li et al. employed a $Fe_2O_3/Ni(OH)_x$ catalyst to produce formic acid and hydrogen from PET via a photoelectrochemical (PEC) process. The PEC process can realize a high FE of ~100% for

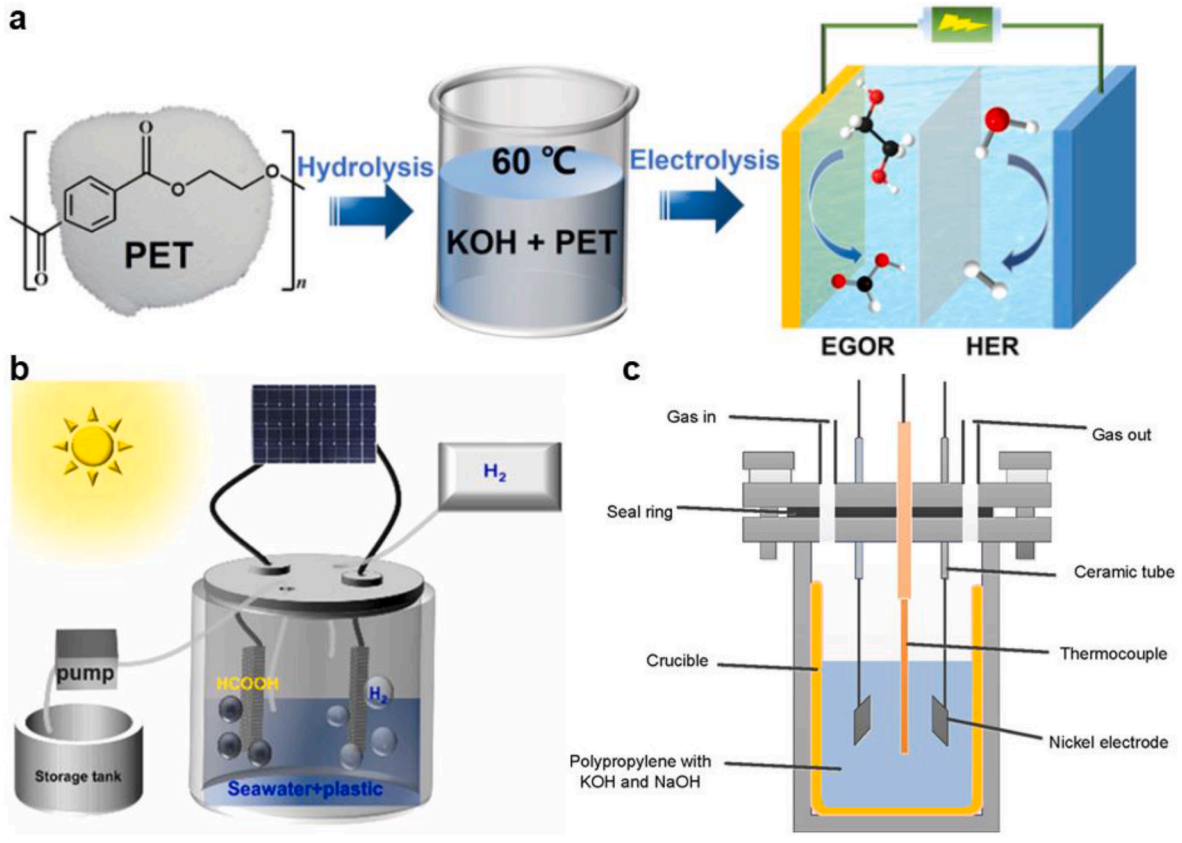

Fig. 14. (a) Scheme of the general PET upcycling and hydrogen production process (EGOR: Ethylene glycol oxidation reaction, HER: hydrogen evolution reaction, PET: polyethylene terephthalate). Reproduced with permission from Ref. [155] Copyright 2023 Springer Nature. (b) Scheme of solar energy-powered hydrogen production and plastics upgrading via electrolysis. Reproduced with permission from Ref. [153] Copyright 2022 Elsevier. (c) Illustration of the solar thermo-coupled electrochemical system for hydrogen production. Reproduced with permission from Ref. [144] Copyright 2020 Elsevier.

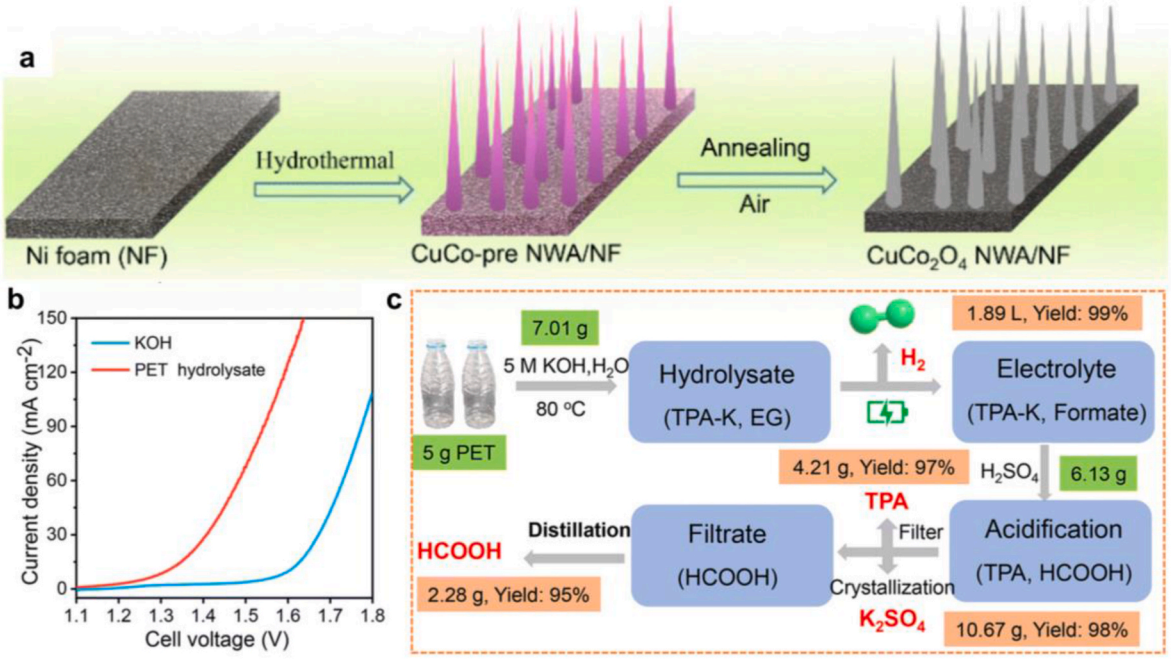

Fig. 15. (a) Scheme of the preparation process of $CuCo_2O_4$ nanowire arrays catalyst. (b) Linear sweep voltammetry curves for $CuCo_2O_4$ catalyst in 5.0 M KOH with and without PET feedstock. (c) Illustration of the electro-reforming and product separation process (EG: ethylene glycol, TPA: terephthalic acid, TPA-K: potassium terephthalate). Reproduced with permission from Ref. [148] Copyright 2022 Royal Society of Chemistry.

formic acid/formate production [172].

Metal nitrides, phosphides, and selenides also attract great interest in plastic waste electro-reforming due to their high conductivity, excellent catalytic activity, and good stability [143,154,156,173,174]. These catalysts generally can be used as bifunctional catalysts for plastic waste electrochemical conversion. Nickel nitrides, like Ni_3N–$Ni_{0.2}Mo_{0.8}N$ [175], Co–Ni_3N [155], and Ni_3N/W_5N_4 [153] have shown promising bifunctional performance toward the electro-reforming of plastics. For instance, the Ni_3N–$Ni_{0.2}Mo_{0.8}N$ nanowire arrays prepared by a solvothermal-calcination method can efficiently catalyze HER and glycerol oxidation reaction (GOR), with a high FE of 96% for formate production. In addition, the Ni_3N–$Ni_{0.2}Mo_{0.8}N$ driven two-electrode electrolyzer for GOR-assisted hydrogen production can attain 10 mA cm^{-2} at 1.40 V, significantly lower than that of conventional alkaline water electrolysis (1.62 V) [175]. Cobalt/nickel phosphides with diverse nanostructures have been designed [154,176]. The Ni-doped CoP (OMS-Ni_1-CoP) with an ordered macroporous structure was synthesized by a three-step process. The unique polyhedral morphology and ordered macroporous superstructure of OMS-Ni_1-CoP would benefit the electrochemical kinetics. In a two-electrode electrolysis reactor for formate and hydrogen production, the bifunctional OMS-Ni_1-CoP catalyst outperforms the noble metals-based electrodes and achieves high FEs for hydrogen (~100 %) and formate (over 80%) production over a wide potential range [176]. These transition metals-based electrocatalysts largely promote the development of plastic waste upcycling and make the plastic-to-hydrogen conversion more sustainable. Nevertheless, current attempts are still limited to several catalysts, and how to improve the catalytic efficiency and selectivity (for value-added formate production) remains an ongoing challenge.

5. Conclusions and perspectives

Upcycling waste plastics into hydrogen fuel is of high environmental and economic interest. Thermochemical, photocatalytic, and electrocatalytic processes have great potential for realizing plastic-to-hydrogen conversion. Currently, sustainable and large-scale plastic-to-hydrogen conversion remains challenging, and some aspects of this field need further exploration. Different from photocatalytic/electrocatalytic processes that can produce high-purity hydrogen gas, the thermochemical process generally produces hydrogen-bearing syngas. The syngas with inconsistent compositions during the reaction process needs to be further regulated to meet the utilization requirements. Alternatively, a hydrogen separation process is required to gain pure hydrogen from the gas mixture. In the thermochemical process, co-pyrolysis or co-gasification of plastics with other wastes (e.g., biowastes, MSW) has been well demonstrated, and some studies have revealed a synergistic effect regarding syngas production and energy efficiency in the co-treatment process. However, the molecular-level reason for the enhancement is complex and how the reaction reactants/intermediates improve the pyrolysis/gasification processes remains poorly understood.

The development of cost-effective catalysts for plastic-to-hydrogen conversion remains a bottleneck. Further studies are suggested to design catalysts based on catalysts' structure-performance relationship. Another issue is that the catalyst-dependent plastic decomposition mechanism remains unclear, and careful investigations based on experimental and computational tools are required. In addition, a group of earth-abundant materials has been implemented for catalytic applications, such as natural ores and biochar, and further efforts are suggested to enhance their catalytic performance. The high energy cost limits the development of thermochemical and electrocatalytic techniques, and it is favorable to integrate solar energy systems into the conversion process. A such combination would largely decrease hydrogen production costs and limit the negative environmental effects of the conventional thermochemical and electrocatalytic techniques. It is also suggested to collect and utilize industrial waste heat as the energy source. Finally, photo- and electro-reforming processes which hold the promise of sustainably producing pure hydrogen fuel from plastic wastes are still in their infancy. More efforts are thus encouraged to expand the photo- and electro-reforming research direction by investigating diverse plastic feedstocks, constructing large-scale reaction systems, designing cost-effective catalysts, and understanding catalytic mechanisms.

Credit author statement

Zhijie Chen: Conceptualization, writing - original draft. **Wei Wei**: Funding acquisition, writing - review & editing. **Xueming Chen**: Writing - review & editing. **Yiwen Liu**: Writing - review & editing. **Yansong Shen**: Writing - review & editing. **Bing-Jie Ni**: Conceptualization, funding acquisition, writing - review & editing.

Declaration of competing interest

The authors declare that they have no known competing financial interests or personal relationships that could have appeared to influence the work reported in this paper.

Data availability

Data will be made available on request.

Acknowledgements

This work is supported by the Australian Research Council (ARC) Discovery Project (DP220101139). Dr. Wei Wei acknowledges the support of the Australian Research Council (ARC) through Project DE220100530.

References

[1] Mitrano DM, Wagner M. A sustainable future for plastics considering material safety and preserved value. Nat Rev Mater 2021;7:71–3.
[2] Hu K, Tian W, Yang Y, Nie G, Zhou P, Wang Y, et al. Microplastics remediation in aqueous systems: Strategies and technologies. Water Res 2021;198:117144.
[3] Mirkarimi SMR, Bensaid S, Chiaramonti D. Conversion of mixed waste plastic into fuel for diesel engines through pyrolysis process: a review. Appl Energy 2022; 327:120040.
[4] Sun J, Dai X, Wang Q, van Loosdrecht MCM, Ni BJ. Microplastics in wastewater treatment plants: Detection, occurrence and removal. Water Res 2019;152:21–37.
[5] Hu K, Yang Y, Zuo J, Tian W, Wang Y, Duan X, et al. Emerging microplastics in the environment: properties, distributions, and impacts. Chemosphere 2022;297: 134118.
[6] Yuan X, Wang X, Sarkar B, Ok YS. The COVID-19 pandemic necessitates a shift to a plastic circular economy. Nat Rev Earth Environ 2021;2:659–60.
[7] Tejaswini MSSR, Pathak P, Ramkrishna S, Ganesh PS. A comprehensive review on integrative approach for sustainable management of plastic waste and its associated externalities. Sci Total Environ 2022;825:153973.
[8] Shi X, Chen Z, Wu L, Wei W, Ni B-J. Microplastics in municipal solid waste landfills: detection, formation and potential environmental risks. Curr Opin Environ Sci Health 2022;31:100433.
[9] Shi X, Chen Z, Wei W, Chen J, Ni B-J. Toxicity of micro/nanoplastics in the environment: roles of plastisphere and eco-corona. Soil Environ Health 2023;1: 100002.
[10] Muhyuddin M, Mustarelli P, Santoro C. Recent advances in waste plastic transformation into valuable platinum-group metal-free electrocatalysts for oxygen reduction reaction. ChemSusChem 2021;14:3785–800.
[11] Chen Z, Wei W, Ni B-J, Chen H. Plastic wastes derived carbon materials for green energy and sustainable environmental applications. Environ Funct Mater 2022;1: 34–48.
[12] Chen Z, Wei W, Liu X, Ni B-J. Emerging electrochemical techniques for identifying and removing micro/nanoplastics in urban waters. Water Res 2022; 221:118846.
[13] Chen Z, Wei W, Shon HK, Ni B-J. Designing bifunctional catalysts for urea electrolysis: progress and perspectives. Green Chem 2024;26:631–54.
[14] Huo E, Lei H, Liu C, Zhang Y, Xin L, Zhao Y, et al. Jet fuel and hydrogen produced from waste plastics catalytic pyrolysis with activated carbon and MgO. Sci Total Environ 2020;727:138411.
[15] Aminu I, Nahil MA, Williams PT. Hydrogen production by pyrolysis–nonthermal plasma/catalytic reforming of waste plastic over different catalyst support materials. Energy Fuel 2022;36:3788–801.
[16] Tang J-H, Sun Y. Visible-light-driven organic transformations integrated with H 2 production on semiconductors. Mater Adv 2020;1:2155–62.
[17] Vollmer I, Jenks MJ, Roelands MC, White RJ, van Harmelen T, de Wild P, et al. Beyond mechanical recycling: giving new life to plastic waste. Angew Chem Int Ed 2020;59:15402–23.
[18] Beliaeva K, Grimaldos-Osorio N, Ruiz-López E, Burel L, Vernoux P, Caravaca A. New insights into lignin electrolysis on nickel-based electrocatalysts: electrochemical performances before and after oxygen evolution. Int J Hydrogen Energy 2021;46:35752–64.
[19] Chen H, Wan K, Zhang Y, Wang Y. Waste to wealth: chemical recycling and chemical upcycling of waste plastics for a great future. ChemSusChem 2021;14: 4123–36.
[20] Zhuo C, Levendis YA. Upcycling waste plastics into carbon nanomaterials: a review. J Appl Polym Sci 2014;131. https://doi.org/10.1002/app.39931.
[21] Karimi Estahbanati MR, Kong XY, Eslami A, Soo HS. Current developments in the chemical upcycling of waste plastics using alternative energy sources. ChemSusChem 2021;14:4152–66.
[22] Ragauskas AJ, Huber GW, Wang J, Guss A, O'Neill HM, Lin CSK, et al. New technologies are needed to improve the recycling and upcycling of waste plastics. ChemSusChem 2021;14:3982.
[23] Hou Q, Zhen M, Qian H, Nie Y, Bai X, Xia T, et al. Upcycling and catalytic degradation of plastic wastes. Cell Rep Phys Sci 2021;2:100514.
[24] Choi J, Yang I, Kim SS, Cho SY, Lee S. Upcycling plastic waste into high value-added carbonaceous materials. Macromol Rapid Commun 2022;43:2100467.
[25] Wang C, Han H, Wu Y, Astruc D. Nanocatalyzed upcycling of the plastic wastes for a circular economy. Coord Chem Rev 2022;458:214422.
[26] Zhang C, Kang Q, Chu M, He L, Chen J. Solar-driven catalytic plastic upcycling. Trends Chem 2022;4:822–34.
[27] Jehanno C, Alty JW, Roosen M, De Meester S, Dove AP, Chen EY-X, et al. Critical advances and future opportunities in upcycling commodity polymers. Nature 2022;603:803–14.
[28] Nanda S, Berruti F. Thermochemical conversion of plastic waste to fuels: a review. Environ Chem Lett 2021;19:123–48.
[29] Williams PT. Hydrogen and carbon nanotubes from pyrolysis-catalysis of waste plastics: a review. Waste Biomass Valorization 2020;12:1–28.
[30] Midilli A, Kucuk H, Haciosmanoglu M, Akbulut U, Dincer I. A review on converting plastic wastes into clean hydrogen via gasification for better sustainability. Int J Energy Res 2022;46:4001–32.
[31] Alam SS, Husain Khan A, Khan NA. Plastic waste management via thermochemical conversion of plastics into fuel: a review. Energy Sources, Part A 2022;44:1–20.
[32] Yao D, Yang H, Chen H, Williams PT. Co-precipitation, impregnation and so-gel preparation of Ni catalysts for pyrolysis-catalytic steam reforming of waste plastics. Appl Catal, B 2018;239:565–77.
[33] Nahil MA, Wu C, Williams PT. Influence of metal addition to Ni-based catalysts for the co-production of carbon nanotubes and hydrogen from the thermal processing of waste polypropylene. Fuel Process Technol 2015;130:46–53.
[34] Barbarias I, Lopez G, Alvarez J, Artetxe M, Arregi A, Bilbao J, et al. A sequential process for hydrogen production based on continuous HDPE fast pyrolysis and in-line steam reforming. Chem Eng J 2016;296:191–8.
[35] Xiao H, Harding J, Lei S, Chen W, Xia S, Cai N, et al. Hydrogen and aromatics recovery through plasma-catalytic pyrolysis of waste polypropylene. J Cleaner Prod 2022;350:131467.
[36] Wang H, Zhang B, Luo P, Huang K, Zhou Y. Simultaneous achievement of high-yield hydrogen and high-performance microwave absorption materials from microwave catalytic deconstruction of plastic waste. Processes 2022;10:782.
[37] Wang J, Pan Y, Song J, Huang Q. A high-quality hydrogen production strategy from waste plastics through microwave-assisted reactions with heterogeneous bimetallic iron/nickel/cerium catalysts. J Anal Appl Pyrolysis 2022;166:105612.
[38] Yang R-X, Wu S-L, Chuang K-H, Wey M-Y. Co-production of carbon nanotubes and hydrogen from waste plastic gasification in a two-stage fluidized catalytic bed. Renew Energy 2020;159:10–22.
[39] Wang J, Cheng G, You Y, Xiao B, Liu S, He P, et al. Hydrogen-rich gas production by steam gasification of municipal solid waste (MSW) using NiO supported on modified dolomite. Int J Hydrogen Energy 2012;37:6503–10.
[40] Lazzarotto IP, Ferreira SD, Junges J, Bassanesi GR, Manera C, Perondi D, et al. The role of CaO in the steam gasification of plastic wastes recovered from the municipal solid waste in a fluidized bed reactor. Process Saf Environ Prot 2020; 140:60–7.
[41] Bian C, Zhang R, Dong L, Bai B, Li W, Jin H, et al. Hydrogen/methane production from supercritical water gasification of lignite coal with plastic waste blends. Energy Fuel 2020;34:11165–74.
[42] Nanda S, Reddy SN, Hunter HN, Vo D-VN, Kozinski JA, Gökalp I. Catalytic subcritical and supercritical water gasification as a resource recovery approach from waste tires for hydrogen-rich syngas production. J Supercrit Fluids 2019; 154:104627.
[43] Cao C, Bian C, Wang G, Bai B, Xie Y, Jin H. Co-gasification of plastic wastes and soda lignin in supercritical water. Chem Eng J 2020;388:124277.
[44] Tabu B, Akers K, Yu P, Baghirzade M, Brack E, Drew C, et al. Nonthermal atmospheric plasma reactors for hydrogen production from low-density polyethylene. Int J Hydrogen Energy 2022;47:39743–57.
[45] Ma W, Chu C, Wang P, Guo Z, Lei S, Zhong L, et al. Hydrogen-rich syngas production by DC thermal plasma steam gasification from biomass and plastic mixtures. Adv Sustainable Syst 2020;4:2000026.
[46] Tang Y, Dong J, Zhao Y, Li G, Chi Y, Weiss-Hortala E, et al. Hydrogen-rich and clean fuel gas production from Co-pyrolysis of biomass and plastic blends with CaO additive. ACS Omega 2022;7:36468–78.
[47] Anuar Sharuddin SD, Abnisa F, Wan Daud WMA, Aroua MK. A review on pyrolysis of plastic wastes. Energy Conv Manag 2016;115:308–26.
[48] Santamaria L, Lopez G, Fernandez E, Cortazar M, Arregi A, Olazar M, et al. Progress on catalyst development for the steam reforming of biomass and waste plastics pyrolysis volatiles: a review. Energy Fuel 2021;35:17051–84.
[49] Zhang Y, Huang J, Williams PT. Fe–Ni–MCM-41 catalysts for hydrogen-rich syngas production from waste plastics by pyrolysis–catalytic steam reforming. Energy Fuel 2017;31:8497–504.

[50] Wu C, Nahil MA, Miskolczi N, Huang J, Williams PT. Production and application of carbon nanotubes, as a co-product of hydrogen from the pyrolysis-catalytic reforming of waste plastic. Process Saf Environ Prot 2016;103:107–14.
[51] Akubo K, Nahil MA, Williams PT. Co-pyrolysis–catalytic steam reforming of cellulose/lignin with polyethylene/polystyrene for the production of hydrogen. Waste Disposal Sustainable Energy 2020;2:177–91.
[52] Yao D, Yang H, Chen H, Williams PT. Investigation of nickel-impregnated zeolite catalysts for hydrogen/syngas production from the catalytic reforming of waste polyethylene. Appl Catal, B 2018;227:477–87.
[53] Nabgan W, Nabgan B, Tuan Abdullah TA, Ikram M, Jadhav AH, Ali MW, et al. Hydrogen and value-added liquid fuel generation from pyrolysis-catalytic steam reforming conditions of microplastics waste dissolved in phenol over bifunctional Ni-Pt supported on Ti-Al nanocatalysts. Catal Today 2022;400–401:35–48.
[54] Namioka T, Saito A, Inoue Y, Park Y, Min T-j, Roh S-A, et al. Hydrogen-rich gas production from waste plastics by pyrolysis and low-temperature steam reforming over a ruthenium catalyst. Appl Energy 2011;88:2019–26.
[55] Park Y, Namioka T, Sakamoto S, Min T-J, Roh S-A, Yoshikawa K. Optimum operating conditions for a two-stage gasification process fueled by polypropylene by means of continuous reactor over ruthenium catalyst. Fuel Process Technol 2010;91:951–7.
[56] Barbarias I, Lopez G, Artetxe M, Arregi A, Bilbao J, Olazar M. Valorisation of different waste plastics by pyrolysis and in-line catalytic steam reforming for hydrogen production. Energy Conv Manag 2018;156:575–84.
[57] Lopez G, Artetxe M, Amutio M, Bilbao J, Olazar M. Thermochemical routes for the valorization of waste polyolefinic plastics to produce fuels and chemicals. A review. Renew Sust Energ Rev 2017;73:346–68.
[58] Arregi A, Seifali Abbas-Abadi M, Lopez G, Santamaria L, Artetxe M, Bilbao J, et al. CeO2 and La2O3 promoters in the steam reforming of polyolefinic waste plastic pyrolysis volatiles on Ni-based catalysts. ACS Sustainable Chem Eng 2020;8:17307–21.
[59] Miandad R, Barakat MA, Aburiazaiza AS, Rehan M, Nizami AS. Catalytic pyrolysis of plastic waste: a review. Process Saf Environ Prot 2016;102:822–38.
[60] Liu X, Tian K, Chen Z, Wei W, Xu B, Ni B-J. Online TG-FTIR-MS analysis of the catalytic pyrolysis of polyethylene and polyvinyl chloride microplastics. J Hazard Mater 2023;441:129881.
[61] Budsaereechai S, Hunt AJ, Ngernyen Y. Catalytic pyrolysis of plastic waste for the production of liquid fuels for engines. RSC Adv 2019;9:5844–57.
[62] Xiao H, Li S, Shi Z, Cui C, Xia S, Chen Y, et al. Plasma-catalytic pyrolysis of polypropylene for hydrogen and carbon nanotubes: understanding the influence of plasma on volatiles. Appl Energy 2023;351:121848.
[63] Chen Z, Monzavi M, Latifi M, Samih S, Chaouki J. Microwave-responsive SiC foam@zeolite core-shell structured catalyst for catalytic pyrolysis of plastics. Environ Pollut 2022;307:119573.
[64] Tyagi VK, Lo S-L. Microwave irradiation: a sustainable way for sludge treatment and resource recovery. Renew Sust Energ Rev 2013;18:288–305.
[65] Putra PHM, Rozali S, Patah MFA, Idris A. A review of microwave pyrolysis as a sustainable plastic waste management technique. J Environ Manage 2022;303:114240.
[66] Jie X, Li W, Slocombe D, Gao Y, Banerjee I, Gonzalez-Cortes S, et al. Microwave-initiated catalytic deconstruction of plastic waste into hydrogen and high-value carbons. Nat Catal 2020;3:902–12.
[67] Yuwen C, Liu B, Rong Q, Hou K, Zhang L, Guo S. Mechanism of microwave-assisted iron-based catalyst pyrolysis of discarded COVID-19 masks. Waste Manage (Tucson, Ariz) 2023;155:77–86.
[68] Fan L, Zhang Y, Liu S, Zhou N, Chen P, Liu Y, et al. Ex-situ catalytic upgrading of vapors from microwave-assisted pyrolysis of low-density polyethylene with MgO. Energy Conv Manag 2017;149:432–41.
[69] Fan L, Liu L, Xiao Z, Su Z, Huang P, Peng H, et al. Comparative study of continuous-stirred and batch microwave pyrolysis of linear low-density polyethylene in the presence/absence of HZSM-5. Energy 2021;228:120612.
[70] Fan L, Su Z, Wu J, Xiao Z, Huang P, Liu L, et al. Integrating continuous-stirred microwave pyrolysis with ex-situ catalytic upgrading for linear low-density polyethylene conversion: effects of parameter conditions. J Anal Appl Pyrolysis 2021;157:105213.
[71] Ding K, Liu S, Huang Y, Liu S, Zhou N, Peng P, et al. Catalytic microwave-assisted pyrolysis of plastic waste over NiO and HY for gasoline-range hydrocarbons production. Energy Conv Manag 2019;196:1316–25.
[72] Chen C, Fan D, Zhao J, Qi Q, Huang X, Zeng T, et al. Study on microwave-assisted co-pyrolysis and bio-oil of Chlorella vulgaris with high-density polyethylene under activated carbon. Energy 2022;247:123508.
[73] Sridevi V, Suriapparao DV, Tukarambai M, Terapalli A, Ramesh P, Sankar Rao C, et al. Understanding of synergy in non-isothermal microwave-assisted in-situ catalytic co-pyrolysis of rice husk and polystyrene waste mixtures. Bioresour Technol 2022;360:127589.
[74] Suriapparao DV, Kumar DA, Vinu R. Microwave co-pyrolysis of PET bottle waste and rice husk: effect of plastic waste loading on product formation. Sustainable Energy Technol Assess 2022;49:101781.
[75] Saebea D, Ruengrit P, Arpornwichanop A, Patcharavorachot Y. Gasification of plastic waste for synthesis gas production. Energy Rep 2020;6:202–7.
[76] Lopez G, Artetxe M, Amutio M, Alvarez J, Bilbao J, Olazar M. Recent advances in the gasification of waste plastics. A critical overview. Renew Sust Energ Rev 2018;82:576–96.
[77] Zhao J, Xie D, Wang S, Zhang R, Wu Z, Meng H, et al. Hydrogen-rich syngas produced from co-gasification of municipal solid waste and wheat straw in an oxygen-enriched air fluidized bed. Int J Hydrogen Energy 2021;46:18051–63.
[78] Mastellone ML, Zaccariello L, Santoro D, Arena U. The O_2-enriched air gasification of coal, plastics and wood in a fluidized bed reactor. Waste Manage (Tucson, Ariz) 2012;32:733–42.
[79] Toledo JM, Aznar MP, Sancho JA. Catalytic air gasification of plastic waste (Polypropylene) in a fluidized bed. Part II: effects of some operating variables on the quality of the raw gas produced using olivine as the in-bed material. Ind Eng Chem Res 2011;50:11815–21.
[80] Sancho JA, Aznar MP, Toledo JM. Catalytic air gasification of plastic waste (polypropylene) in fluidized bed. Part I: use of in-gasifier bed additives. Ind Eng Chem Res 2008;47:1005–10.
[81] Xiao R, Jin B, Zhou H, Zhong Z, Zhang M. Air gasification of polypropylene plastic waste in fluidized bed gasifier. Energy Conv Manag 2007;48:778–86.
[82] Arena U, Di Gregorio F. Energy generation by air gasification of two industrial plastic wastes in a pilot scale fluidized bed reactor. Energy 2014;68:735–43.
[83] Yang R-X, Chuang K-H, Wey M-Y. Effects of temperature and equivalence ratio on carbon nanotubes and hydrogen production from waste plastic gasification in fluidized bed. Energy Fuel 2018;32:5462–70.
[84] Yang R-X, Chuang K-H, Wey M-Y. Carbon nanotube and hydrogen production from waste plastic gasification over Ni/Al–SBA-15 catalysts: effect of aluminum content. RSC Adv 2016;6:40731–40.
[85] Yang R-X, Chuang K-H, Wey M-Y. Effects of nickel species on Ni/Al_2O_3 catalysts in carbon nanotube and hydrogen production by waste plastic gasification: bench- and pilot-scale tests. Energy Fuel 2015;29:8178–87.
[86] Cho M-H, Choi Y-K, Kim J-S. Air gasification of PVC (polyvinyl chloride)-containing plastic waste in a two-stage gasifier using Ca-based additives and Ni-loaded activated carbon for the production of clean and hydrogen-rich producer gas. Energy 2015;87:586–93.
[87] Cho M-H, Mun T-Y, Kim J-S. Air gasification of mixed plastic wastes using calcined dolomite and activated carbon in a two-stage gasifier to reduce tar. Energy 2013;53:299–305.
[88] Cho M-H, Mun T-Y, Kim J-S. Production of low-tar producer gas from air gasification of mixed plastic waste in a two-stage gasifier using olivine combined with activated carbon. Energy 2013;58:688–94.
[89] Cho M-H, Mun T-Y, Choi Y-K, Kim J-S. Two-stage air gasification of mixed plastic waste: olivine as the bed material and effects of various additives and a nickel-plated distributor on the tar removal. Energy 2014;70:128–34.
[90] Jeong Y-S, Choi Y-K, Kim J-S. Three-stage air gasification of waste polyethylene: in-situ regeneration of active carbon used as a tar removal additive. Energy 2019;166:335–42.
[91] Jeong Y-S, Kim J-W, Seo M-W, Mun T-Y, Kim J-S. Characteristics of two-stage air gasification of polystyrene with active carbon as a tar removal agent. Energy 2021;219:119681.
[92] Kim J-W, Mun T-Y, Kim J-O, Kim J-S. Air gasification of mixed plastic wastes using a two-stage gasifier for the production of producer gas with low tar and a high caloric value. Fuel 2011;90:2266–72.
[93] Jeong Y-S, Kim J-W, Ra HW, Seo MW, Mun T-Y, Kim J-S. Characteristics of air gasification of 10 different types of plastic in a two-stage gasification process. ACS Sustainable Chem Eng 2022;10:4705–16.
[94] Choi M-J, Jeong Y-S, Kim J-S. Air gasification of polyethylene terephthalate using a two-stage gasifier with active carbon for the production of H_2 and CO. Energy 2021;223:120122.
[95] Erkiaga A, Lopez G, Amutio M, Bilbao J, Olazar M. Syngas from steam gasification of polyethylene in a conical spouted bed reactor. Fuel 2013;109:461–9.
[96] Kamo T, Takaoka K, Otomo J, Takahashi H. Production of hydrogen by steam gasification of dehydrochlorinated poly (vinyl chloride) or activated carbon in the presence of various alkali compounds. J Mater Cycles Waste Manag 2006;8:109–15.
[97] Burra KG, Gupta AK. Synergistic effects in steam gasification of combined biomass and plastic waste mixtures. Appl Energy 2018;211:230–6.
[98] Lopez G, Erkiaga A, Amutio M, Bilbao J, Olazar M. Effect of polyethylene co-feeding in the steam gasification of biomass in a conical spouted bed reactor. Fuel 2015;153:393–401.
[99] Lee U, Chung JN, Ingley HA. High-temperature steam gasification of municipal solid waste, rubber, plastic and wood. Energy Fuel 2014;28:4573–87.
[100] Salbidegoitia JA, Fuentes-Ordóñez EG, González-Marcos MP, González-Velasco JR, Bhaskar T, Kamo T. Steam gasification of printed circuit board from e-waste: effect of coexisting nickel to hydrogen production. Fuel Process Technol 2015;133:69–74.
[101] Lopez G, Erkiaga A, Artetxe M, Amutio M, Bilbao J, Olazar M. Hydrogen production by high density polyethylene steam gasification and in-line volatile reforming. Ind Eng Chem Res 2015;54:9536–44.
[102] Wilk V, Hofbauer H. Conversion of mixed plastic wastes in a dual fluidized bed steam gasifier. Fuel 2013;107:787–99.
[103] Farooq A, Moogi S, Jang S-H, Kannapu HPR, Valizadeh S, Ahmed A, et al. Linear low-density polyethylene gasification over highly active Ni/CeO_2-ZrO_2 catalyst for enhanced hydrogen generation. J Ind Eng Chem 2021;94:336–42.
[104] Okolie JA, Nanda S, Dalai AK, Berruti F, Kozinski JA. A review on subcritical and supercritical water gasification of biogenic, polymeric and petroleum wastes to hydrogen-rich synthesis gas. Renew Sust Energ Rev 2020;119:109546.
[105] Lu B, Bai B, Zhang R, Ma J, Mao L, Shi J, et al. Study on gasification characteristics and kinetics of polyformaldehyde plastics in supercritical water. J Cleaner Prod 2023;383:135459.
[106] Bai B, Wang W, Jin H. Experimental study on gasification performance of polypropylene (PP) plastics in supercritical water. Energy 2020;191:116527.

[107] Wang W, Bai B, Wei W, Cao C, Jin H. Hydrogen-rich syngas production by gasification of Urea-formaldehyde plastics in supercritical water. Int J Hydrogen Energy 2021;46:35121–9.

[108] Su H, Liao W, Wang J, Hantoko D, Zhou Z, Feng H, et al. Assessment of supercritical water gasification of food waste under the background of waste sorting: influences of plastic waste contents. Int J Hydrogen Energy 2020;45:21138–47.

[109] Chen J, Fu L, Tian M, Kang S, E J. Comparison and synergistic effect analysis on supercritical water gasification of waste thermoplastic plastics based on orthogonal experiments. Energy 2022;261:125104.

[110] Onwudili JA, Williams PT. Catalytic supercritical water gasification of plastics with supported RuO_2: a potential solution to hydrocarbons–water pollution problem. Process Saf Environ Prot 2016;102:140–9.

[111] Nanda S, Okolie JA, Patel R, Pattnaik F, Fang Z, Dalai AK, et al. Catalytic hydrothermal co-gasification of canola meal and low-density polyethylene using mixed metal oxides for hydrogen production. Int J Hydrogen Energy 2022;47:42084–98.

[112] Li J, Pan L, Suvarna M, Wang X. Machine learning aided supercritical water gasification for H_2-rich syngas production with process optimization and catalyst screening. Chem Eng J 2021;426:131285.

[113] Mallick R, Vairakannu P. Experimental investigation of acrylonitrile butadiene styrene plastics plasma gasification. J Environ Manage 2023;345:118655.

[114] Mazzoni L, Janajreh I. Plasma gasification of municipal solid waste with variable content of plastic solid waste for enhanced energy recovery. Int J Hydrogen Energy 2017;42:19446–57.

[115] Yun YM, Seo MW, Ra HW, Yoon SJ, Mun T-Y, Moon J-H, et al. Gasification characteristics of glass fiber-reinforced plastic (GFRP) wastes in a microwave plasma reactor. Kor J Chem Eng 2017;34:2756–63.

[116] Hlina M, Hrabovsky M, Kavka T, Konrad M. Production of high quality syngas from argon/water plasma gasification of biomass and waste. Waste Manage (Tucson, Ariz) 2014;34:63–6.

[117] Sikarwar VS, Peela NR, Vuppaladadiyam AK, Ferreira NL, Mašláni A, Tomar R, et al. Thermal plasma gasification of organic waste stream coupled with CO_2-sorption enhanced reforming employing different sorbents for enhanced hydrogen production. RSC Adv 2022;12:6122–32.

[118] Cho IJ, Park H-W, Park D-W, Choi S. Enhancement of synthesis gas production using gasification-plasma hybrid system. Int J Hydrogen Energy 2015;40:1709–16.

[119] Nguyen HM, Carreon ML. Non-thermal plasma-assisted deconstruction of high-density polyethylene to hydrogen and light hydrocarbons over hollow ZSM-5 microspheres. ACS Sustainable Chem Eng 2022;10:9480–91.

[120] Kaushal R, Rohit, Dhaka AK. A comprehensive review of the application of plasma gasification technology in circumventing the medical waste in a post-COVID-19 scenario. Biomass Convers Biorefin 2022. https://doi.org/10.1007/s13399-022-02434-z.

[121] Liu F, Zhuang X, Du Z, Dan Y, Huang Y, Jiang L. Enhanced photocatalytic performance by polarizing ferroelectric $KNbO_3$ for degradation of plastic wastes under mild conditions. Appl Catal, B 2022;318:121897.

[122] Shi X, Chen Z, Liu X, Wei W, Ni B-J. The photochemical behaviors of microplastics through the lens of reactive oxygen species: photolysis mechanisms and enhancing photo-transformation of pollutants. Sci Total Environ 2022;846:157498.

[123] Du M, Zhang Y, Kang S, Guo X, Ma Y, Xing M, et al. Trash to treasure: photoreforming of plastic waste into commodity chemicals and hydrogen over MoS_2-tipped CdS nanorods. ACS Catal 2022;12:12823–32.

[124] Zhao L, Dong T, Du J, Liu H, Yuan H, Wang Y, et al. Synthesis of CdS/MoS_2 nanooctahedrons heterostructure with a tight interface for enhanced photocatalytic H_2 evolution and biomass upgrading. Sol RRL 2021;5:2000415.

[125] Cao B, Wan S, Wang Y, Guo H, Ou M, Zhong Q. Highly-efficient visible-light-driven photocatalytic H_2 evolution integrated with microplastic degradation over MXene/$Zn_xCd_{1-x}S$ photocatalyst. J Colloid Interface Sci 2022;605:311–9.

[126] Uekert T, Kuehnel MF, Wakerley DW, Reisner E. Plastic waste as a feedstock for solar-driven H 2 generation. Energy Environ Sci 2018;11:2853–7.

[127] Nagakawa H, Nagata M. Photoreforming of organic waste into hydrogen using a thermally radiative CdO_x/CdS/SiC photocatalyst. ACS Appl Mater Interfaces 2021;13:47511–9.

[128] Han M, Zhu S, Xia C, Yang B. Photocatalytic upcycling of poly(ethylene terephthalate) plastic to high-value chemicals. Appl Catal, B 2022;316:121662.

[129] Sun D-W, Chen K-L, Huang J-H. Benzenesulfonyl chloride-incorporated g-C_3N_4 for photocatalytic hydrogen generation by using the hydrolysate of poly(lactic acid) as sacrificial reagent. Appl Catal A 2021;628:118397.

[130] Yan J-Q, Sun D-W, Huang J-H. Synergistic poly(lactic acid) photoreforming and H_2 generation over ternary $Ni_xCo_{1-x}P$/reduced graphene oxide/g-C_3N_4 composite. Chemosphere 2022;286:131905.

[131] Qin J, Dou Y, Wu F, Yao Y, Andersen HR, Hélix-Nielsen C, et al. In-situ formation of Ag_2O in metal-organic framework for light-driven upcycling of microplastics coupled with hydrogen production. Appl Catal, B 2022;319:121940.

[132] Gogoi R, Singh A, Moutam V, Sharma L, Sharma K, Halder A, et al. Revealing the unexplored effect of residual iron oxide on the photoreforming activities of polypyrrole nanostructures on plastic waste and photocatalytic pollutant degradation. J Environ Chem Eng 2022;10:106649.

[133] Gong X, Tong F, Ma F, Zhang Y, Zhou P, Wang Z, et al. Photoreforming of plastic waste poly (ethylene terephthalate) via in-situ derived CN-CNTs-NiMo hybrids. Appl Catal, B 2022;307:121143.

[134] Dai W, Wang R, Chen Z, Deng S, Huang C, Luo W, et al. Highly-efficient photocatalytic hydrogen evolution triggered by spatial confinement effects over co-crystal templated boron-doped carbon nitride hollow nanotubes. J Mater Chem A 2023;11:7584–95.

[135] Huang W, Bo T, Zuo S, Wang Y, Chen J, Ould-Chikh S, et al. Surface decorated Ni sites for superior photocatalytic hydrogen production. SusMat 2022;2:466–75.

[136] Chu S, Zhang B, Zhao X, Soo HS, Wang F, Xiao R, et al. Photocatalytic conversion of plastic waste: from photodegradation to photosynthesis. Adv Energy Mater 2022;12:2200435.

[137] Hao D, Liu C, Xu X, Kianinia M, Aharonovich I, Bai X, et al. Surface defect-abundant one-dimensional graphitic carbon nitride nanorods boost photocatalytic nitrogen fixation. New J Chem 2020;44:20651–8.

[138] Dai W, Mu J, Chen Z, Zhang J, Pei X, Luo W, et al. Design of few-layer carbon nitride/$BiFeO_3$ composites for efficient organic pollutant photodegradation. Environ Res 2022;215:114190.

[139] Chen Z, Wei W, Chen H, Ni B. Recent advances in waste-derived functional materials for wastewater remediation. Eco-Environ Health 2022;1:86–104.

[140] Uekert T, Bajada MA, Schubert T, Pichler CM, Reisner E. Scalable photocatalyst panels for photoreforming of plastic, biomass and mixed waste in flow. ChemSusChem 2021;14:4190–7.

[141] Uekert T, Kasap H, Reisner E. Photoreforming of nonrecyclable plastic waste over a carbon nitride/nickel phosphide catalyst. J Am Chem Soc 2019;141:15201–10.

[142] Xu J, Jiao X, Zheng K, Shao W, Zhu S, Li X, et al. Plastics-to-syngas photocatalysed by Co–Ga_2O_3 nanosheets. Natl Sci Rev 2022;9:nwac011.

[143] Li Y, Zhao Y, Zhao H, Wang Z, Li H, Gao P. A bifunctional catalyst of ultrathin cobalt selenide nanosheets for plastic-electroreforming-assisted green hydrogen generation. JMater Chem A 2022;10:20446–52.

[144] Jiang T, Zhao X, Gu D, Yan C, Jiang H, Wu H, et al. STEP polymer degradation: solar thermo-coupled electrochemical depolymerization of plastics to generate useful fuel plus abundant hydrogen. Sol Energy Mater Sol Cells 2020;204:110208.

[145] Grimaldos-Osorio N, Sordello F, Passananti M, González-Cobos J, Bonhommé A, Vernoux P, et al. From plastic-waste to H_2: a first approach to the electrochemical reforming of dissolved Poly(methyl methacrylate) particles. Int J Hydrogen Energy 2023;48:11899–913.

[146] Hori T, Kobayashi K, Teranishi S, Nagao M, Hibino T. Fuel cell and electrolyzer using plastic waste directly as fuel. Waste Manage (Tucson, Ariz) 2020;102:30–9.

[147] Grimaldos-Osorio N, Sordello F, Passananti M, Vernoux P, Caravaca A. From plastic-waste to H_2: electrolysis of a Poly(methyl methacrylate) model molecule on polymer electrolyte membrane reactors. J Power Sources 2020;480:228800.

[148] Liu F, Gao X, Shi R, Tse ECM, Chen Y. A general electrochemical strategy for upcycling polyester plastics into added-value chemicals by a $CuCo_2O_4$ catalyst. Green Chem 2022;24:6571–7.

[149] Chen Z, Zheng R, Bao T, Ma T, Wei W, Shen Y, et al. Dual-doped nickel sulfide for electro-upgrading polyethylene terephthalate into valuable chemicals and hydrogen fuel. Nano-Micro Lett 2023;15:210.

[150] Chen Z, Wei W, Shen Y, Ni B-J. Defective nickel sulfide hierarchical structures for efficient electrochemical conversion of plastic waste to value-added chemicals and hydrogen fuel. Green Chem 2023;25:5979–88.

[151] Shi R, Liu K-S, Liu F, Yang X, Hou C-C, Chen Y. Electrocatalytic reforming of waste plastics into high value-added chemicals and hydrogen fuel. Chem Commun 2021;57:12595–8.

[152] Zhang H, Wang Y, Li X, Deng K, Yu H, Xu Y, et al. Electrocatalytic upcycling of polyethylene terephthalate plastic to formic acid coupled with energy-saving hydrogen production over hierarchical Pd-doped NiTe nanoarrays. Appl Catal, B 2024;340:123236.

[153] Ma F, Wang S, Gong X, Liu X, Wang Z, Wang P, et al. Highly efficient electrocatalytic hydrogen evolution coupled with upcycling of microplastics in seawater enabled via Ni_3N/W_5N_4 janus nanostructures. Appl Catal, B 2022;307:121198.

[154] Zhou H, Ren Y, Li Z, Xu M, Wang Y, Ge R, et al. Electrocatalytic upcycling of polyethylene terephthalate to commodity chemicals and H_2 fuel. Nat Commun 2021;12:4679.

[155] Liu X, Fang Z, Xiong D, Gong S, Niu Y, Chen W, et al. Upcycling PET in parallel with energy-saving H2 production via bifunctional nickel-cobalt nitride nanosheets. Nano Res 2023;16:4625–33.

[156] Chen Z, Wei W, Ni B-J. Transition metal chalcogenides as emerging electrocatalysts for urea electrolysis. Curr Opin Electrochem 2022;31:100888.

[157] Chen Z, Wei W, Song L, Ni B-J. Hybrid water electrolysis: a new sustainable avenue for energy-saving hydrogen production. Sustainable Horiz 2022;1:100002.

[158] Du L, Sun Y, You B. Hybrid water electrolysis: replacing oxygen evolution reaction for energy-efficient hydrogen production and beyond. Mater Rep: Energy 2020;1:100004.

[159] Li S, Liu D, Wang G, Ma P, Wang X, Wang J, et al. Vertical 3D nanostructures boost efficient hydrogen production coupled with glycerol oxidation under alkaline conditions. Nano-Micro Lett 2023;15:189.

[160] Chen Z, Zheng R, Zou H, Wang R, Huang C, Dai W, et al. Amorphous iron-doped nickel boride with facilitated structural reconstruction and dual active sites for efficient urea electrooxidation. Chem Eng J 2023;465:142684.

[161] Xiong P, Tan J, Lee H, Ha N, Lee SJ, Yang W, et al. Two-dimensional carbon-based heterostructures as bifunctional electrocatalysts for water splitting and metal–air batteries. Nano Mater Sci 2022. https://doi.org/10.1016/j.nanoms.2022.10.001.

[162] Li X-X, Liu X-C, Liu C, Zeng J-M, Qi X-P. Co_3O_4/stainless steel catalyst with synergistic effect of oxygen vacancies and phosphorus doping for overall water splitting. Tungsten 2023;5:100–8.

[163] You N, Cao S, Huang M, Fan X, Shi K, Huang H, et al. Constructing P-CoMoO4@NiCoP heterostructure nanoarrays on Ni foam as efficient bifunctional electrocatalysts for overall water splitting. Nano Mater Sci 2023;5:278–86.

[164] Chen Z, Zheng R, Zou W, Wei W, Li J, Wei W, et al. Integrating high-efficiency oxygen evolution catalysts featuring accelerated surface reconstruction from waste printed circuit boards via a boriding recycling strategy. Appl Catal, B 2021; 298:120583.
[165] Qian J, Zhang Y, Chen Z, Du Y, Ni B-J. NiCo layered double hydroxides/NiFe layered double hydroxides composite (NiCo-LDH/NiFe-LDH) towards efficient oxygen evolution in different water matrices. Chemosphere 2023;345:140472.
[166] Chen Z, Wei W, Zou W, Li J, Zheng R, Wei W, et al. Integrating electrodeposition with electrolysis for closing loop resource utilization of battery industrial wastewater. Green Chem 2022;44:3208–17.
[167] Guo F, Chen Q, Liu Z, Cheng D, Han N, Chen Z. Repurposing mining and metallurgical waste as electroactive materials for advanced energy applications: advances and perspectives. Catalysts 2023;13:1241.
[168] Chen Z, Duan X, Wei W, Wang S, Ni B-J. Electrocatalysts for acidic oxygen evolution reaction: achievements and perspectives. Nano Energy 2020;78: 105392.
[169] Mu Y, Pei X, Zhao Y, Dong X, Kou Z, Cui M, et al. In situ confined vertical growth of $Co_{2.5}Ni_{0.5}Si_2O_5(OH)_4$ nanoarrays on rGO for an efficient oxygen evolution reaction. Nano Mater Sci 2023;5:351–60.
[170] Cho J, Kim B, Kwon T, Lee K, Choi S-I. Electrocatalytic upcycling of plastic waste. Green Chem 2023;25:8444–58.
[171] Wang J, Li X, Zhang T, Chen Y, Wang T, Zhao Y. Electro-reforming polyethylene terephthalate plastic to Co-produce valued chemicals and green hydrogen. J Phys Chem Lett 2022;13:622–7.
[172] Li X, Wang J, Zhang T, Wang T, Zhao Y. Photoelectrochemical catalysis of waste polyethylene terephthalate plastic to coproduce formic acid and hydrogen. ACS Sustainable Chem Eng 2022;10:9546–52.
[173] Chen Z, Duan X, Wei W, Wang S, Ni B-J. Recent advances in transition metal-based electrocatalysts for alkaline hydrogen evolution. J Mater Chem A 2019;7: 14971–5005.
[174] Chen Z, Han N, Zheng R, Ren Z, Wei W, Ni BJ. Design of earth-abundant amorphous transition metal-based catalysts for electrooxidation of small molecules: advances and perspectives. SusMat 2023;3:290–319.
[175] Liu X, Fang Z, Teng X, Niu Y, Gong S, Chen W, et al. Paired formate and H_2 productions via efficient bifunctional Ni-Mo nitride nanowire electrocatalysts. J Energy Chem 2022;72:432–41.
[176] Wang N, Li X, Hu M-K, Wei W, Zhou S-H, Wu X-T, et al. Ordered macroporous superstructure of bifunctional cobalt phosphide with heteroatomic modification for paired hydrogen production and polyethylene terephthalate plastic recycling. Appl Catal, B 2022;316:121667.